THE EFFECT OF CURING LIGHT DISTANCE ON THE EFFECTIVENESS OF CURE OF BULK-FILL RESIN-BASED COMPOSITES

RANA ABDELBASET LOTFY DIAB

FACULTY OF DENTISTRY
UNIVERSITY OF MALAYA
KUALA LUMPUR

2019

THE EFFECT OF CURING LIGHT DISTANCE ON THE EFFECTIVENESS OF CURE OF BULK-FILL RESIN-BASED COMPOSITES

RANA ABDELBASET LOTFY DIAB

SUPERVISOR: DR. NOOR AZLIN YAHYA

CO-SUPERVISOR: DR. MARIA ANGELA GARCIA GONZALEZ

CO-SUPERVISOR: PROFESSOR DR. ADRIAN YAP U JIN

RESEARCH REPORT SUBMITTED IN PARTIAL FULFILMENT OF THE REQUIREMENTS FOR THE DEGREE OF MCLINDENT IN CONSERVATIVE DENTISTRY

FACULTY OF DENTISTRY
UNIVERSITY OF MALAYA
KUALA LUMPUR

2019

UNIVERSITY OF MALAYA

ORIGINAL LITERARY WORK DECLARATION

Name of Candidate: **Rana Abdelbaset Lotfy Diab**

Matric No: **DGI160005**

Name of Degree: **Master of Clinical Dentistry in Conservative Dentistry in Restorative Dentistry**

Title of Research Report: **The Effect of Curing Light Distance on The Effectiveness of Cure of Bulk-Fill Resin-Based Composites**

Field of Study: **Restorative Dentistry, Dental Materials.**

I do solemnly and sincerely declare that:

(1) I am the sole author/writer of this Work;
(2) This Work is original;
(3) Any use of any work in which copyright exists was done by way of fair dealing and for permitted purposes and any excerpt or extract from, or reference to or reproduction of any copyright work has been disclosed expressly and sufficiently and the title of the Work and its authorship have been acknowledged in this Work;
(4) I do not have any actual knowledge nor do I ought reasonably to know that the making of this work constitutes an infringement of any copyright work;
(5) I hereby assign all and every right in the copyright to this Work to the University of Malaya ("UM"), who henceforth shall be owner of the copyright in this Work and that any reproduction or use in any form or by any means whatsoever is prohibited without the written consent of UM having been first had and obtained;
(6) I am fully aware that if in the course of making this Work I have infringed any copyright whether intentionally or otherwise, I may be subject to legal action or any other action as may be determined by UM.

Candidate's Signature Date: 12th of June, 2019

Subscribed and solemnly declared before,

Witness's Signature Date: 12th of June, 2019

Name:

Designation:

ABSTRACT

Objectives: To investigate the effect of different curing light distances on the surface hardness (SH) and the effectiveness of cure of bulk-fill resin-based composites (RBCs).

Methodology: Two bulk-fill RBCs (Tetric N Ceram® Bulk Fill [TN] and Filtek™ Bulk Fill [FK]) were evaluated. Cylindrical RBC specimens of 5 mm diameter and 4 mm height were fabricated using black Perspex® acrylic moulds. Photopolymerization of the RBC specimens was carried out at different light-curing distances (0 mm, 2 mm, 4 mm, 6 mm and 8 mm) and stored for 24 hours at 37°C in 100% relative humidity. The SH (n=12) of the top and bottom surfaces of each specimen was assessed using a Knoop hardness micro-indentation tester. The bottom to top SH values were calculated to obtain the hardness ratio (HR) for each specimen. HR of the two bulk-fill RBCs were compared.

Results: Data were analysed using one-way ANOVA and Tukey's post hoc test ($\alpha<0.05$). At various curing light distances, the mean SH for TN ranged between 34.45 and 41.24 for the top surface and between 9.12 and 17.56 for the bottom surface. However, for FK, the mean SH ranged from 44.76 to 51.12 and from 32.57 to 37.60 for the top and bottom surfaces respectively. The mean HR values which characterizes the effectiveness of cure ranged from 0.27 to 0.46 for TN and from 0.68 to 0.79 for FK at different curing light distances. The HR of TN at 8 mm curing light distance was significantly lower in comparison to the other curing light distances. However, for FK, 8 mm curing light distance was only significantly lower than that of 0 mm. FK had significantly higher HR than TN at different curing light distances.

Conclusions: The top and bottom SH of TN and FK are affected by the curing light distance. The HR of TN and FK resulted in a linear relationship with the curing light distance. The effectiveness of cure decreased with the increase of the curing light

distance. The effectiveness of cure of bulk-fill resin-based composites is material-dependent.

Keywords: Bulk-fill, Resin-based composites, curing light distance, Surface hardness effectiveness of cure.

ABSTRAK

Objektif: Untuk menyiasat kesan jarak pempolimeran cahaya yang berbeza pada kekerasan permukaan (SH) dan keberkesanan pempolimeran komposit berasaskan resin (RBC) yang berjenis tampal dengan pukal.

Metodologi: Dua RBC yang berjenis tampal dengan pukal (Tetric N-Ceram® [TN] Bulk Fill dan Filtek™ Bulk Fill [FK]) telah dinilaikan. Spesimen RBC yang berbentuk silinder dengan ukuran diameter 5 mm dan ketinggian 4 mm telah dihasilkan dengan menggunakan akrilik Perspex® berwarna hitam. Pempolimeran cahaya pada spesimen RBC dijalankan dengan jarak yang berbeza (0 mm, 2 mm, 4 mm, 6 mm dan 8 mm). Selepas itu, specimen disimpan dalam kelembapan relatif 100% dengan 37°C selama 24 jam. SH (n = 12) permukaan atas dan bawah setiap spesimen dinilai dengan penguji mikro-lekukan kekerasan Knoop. Nisbah SH permukaan bawah kepada SH permukaan atas dikira untuk memperolehi nisbah kekerasan (HR) bagi setiap spesimen. HR kedua-dua jenis RBC telah dibandingkan.

Keputusan: Data dianalisis dengan menggunakan one-way ANOVA dan ujian post hoc Tukey's (α=0.05). Di pelbagai jarak pempolimeran cahaya, purata SH bagi TN adalah di antara 34.45 hingga 41.24 untuk permukaan atas dan di antara 9.12 hingga 17.56 untuk permukaan bawah. Bagi FK, purata SH bagi permukaan atas adalah dari 44.76 hingga 51.12 dan bagi permukaan bawah adalah 32.57 hingga 37.60. Nilai HR yang mewakili keberkesanan pempolimeran adalah di antara 0.27 hingga 0.46 untuk TN dan dari 0.68 hingga 0.79 untuk FK pada jarak cahaya pempolimeran yang berbeza. HR untuk TN pada jarak pempolimeran cahaya 8 mm adalah lebih rendah secara statistik apabila berbanding dengan jarak cahaya pempolimeran yang lain. Bagaimanapun, untuk FK, jarak pempolimeran cahaya pada 8 mm hanya lebih rendah secara statistik daripada 0 mm. FK mempunyai HR yang lebih tinggi secara statistik daripada TN pada semua jarak cahaya pempolimeran yang dinilaikan.

Kesimpulan: SH untuk permukaan atas dan permukaan bawah untuk TN dan FK dipengaruhi oleh jarak cahaya pempolimeran. HR untuk TN dan FK menghasilkan hubungan secara linear dengan jarak cahaya pempolimeran. Keberkesanan pempolimeran menurun apabila peningkatan jarak cahaya pempolimeran. Keberkesanan pempolimeran komposit berasaskan resin yang berjenis tampal dengan pukal adalah bergantung pada jenis bahan yang digunakan.

Kata kunci: Tampal dengan pukal, komposit berasaskan resin, jarak pempolimeran cahaya, kekerasan permukaan, keberkesanan pempolimeran

ACKNOWLEDGEMENTS

I would like to thank my supervisor Dr Noor Azlin Yahya, and my co-supervisors Dr Maria Angela Garcia Gonzalez and Professor Dr Adrian Yap U Jin. If it was not for their support and guidance, I would not have been able to do this research. They were very patient and kind towards me. They consistently allowed this research to be my own work and steered me in the right direction whenever they thought I needed it.

I am grateful to Dr Muralithran A/L Govindan Kutty, a senior lecturer from the Department of Restorative Dentistry, University of Malaya for sharing his expertise and his sincere and valuable guidance.

I wish to express my warm thanks and gratitude to all of the members of Biomaterial Research Laboratory especially Mrs Zarina Bt Idris and Mrs Chanthiriga A/P Ramasindarum for helping me with great kindness and patience during my experiment.

I would like to express my full appreciation and gratefulness for my parents. I would have never made it without their endless love, care, support and motivation. They are the main reason for my hard work and dedication. They sacrificed a lot for me and my daughter. I would also like to thank my beloved brothers, Amr and Khaled who supported me in their own marvellous way. Finally, a special thanks to my source of inspiration, my daughter Jannah, who carried this heavy weight with me.

TABLE OF CONTENTS

LIST OF FIGURES

LIST OF TABLES

LIST OF SYMBOLS AND ABBREVIATIONS

AL	:	Argon-ion lasers
APO	:	Acyl phosphine oxide
B/T-DC	:	bottom to top degree of conversion
B/T-KHN	:	bottom to top Knoop hardness number
B/T-ratio		bottom to top ratio
BAPO	:	bisacylphosphine oxide
BHT	:	2,6-di-tert-butyl-methylphenol
Bis-GMA	:	2,2-bis[4-(2-hydroxy-3-methacrylyloxypropoxy)phenyl]propane
C=C	:	Carbon-carbon double bond
CQ	:	Camphorquinone
DC	:	Degree of conversion
DSC	:	differential scanning calorimetry
DTA	:	differential thermal analysis
EGDMA	:	ethyleneglycol dimethacrylate
FK	:	Filtek™ Bulk Fill
FTIR	:	Fourier Transform Infrared Spectroscopy
HR	:	Hardness Ratio
IR	:	Infrared
KHN	:	Knoop hardness number
LCU	:	Light curing unit
LED	:	Light-emitting diodes
MAPO	:	monoacylphosphine oxide
MEHQ	:	hydroquinone monomethylether
MPTMS	:	(methacryloxy)propyltrimethoxy silane

MRS	:	micro-Raman spectroscopy
NMR	:	nuclear magnetic resonance
PAC	:	Plasma arc curing
PPD	:	phenyl propanedione
PTFE	:	Polytetrafluoroethylene
QTH	:	Quartz tungsten halogen
RBC	:	Resin-based composite
SDR	:	stress decreasing resin
SH	:	Surface hardness
TEGDMA	:	triethylene glycol dimethacrylate
TN	:	Tetric N-Ceram Bulk Fill
TPO	:	2,4,6-trimethylbenzoyldiphenylphosphine oxide
UDMA	:	urethane dimethacrylate
UV	:	Ultraviolet
Vol.%	:	Volume percent
Wt.%	:	Weight percent

LIST OF APPENDICES

CHAPTER 1: INTRODUCTION

Dental resin-based composites (RBCs) are widely used in dental practices due to their excellent aesthetics, high polishability, ability to bond to teeth and good mechanical properties. RBCs have been significantly improved since they were first introduced in the 1950s through innovations in photoinitiator, polymeric matrix, filler type and size (Ferracane, 2011). Despite the advances made in RBC technology, polymerization shrinkage and incomplete photopolymerization remain problematic. Polymerization shrinkage leads to contraction of total RBC volume resulting in internal stresses, voids and cracks within the restoration, de-bonding, marginal leakage, postoperative sensitivity and secondary caries (Braga, Boaro, Kuroe, Azevedo, & Singer, 2006; Eick & Welch, 1986; Feilzer, De Gee, & Davidson, 1987). Conversely, incomplete photopolymerization impacts the mechanical properties of RBCs as well as their solubility, dimensional constancy, colour stability and biocompatibility (Sobrinho, Goes, Consani, Sinhoreti, & Knowles, 2000).

In an attempt to mitigate these problems, the incremental technique of RBC placement was introduced. This involves the application of RBC materials in layers of 1.5mm to 2mm thickness (Davidson, 1986). The concept has been accepted for years and allows for better photopolymerization and reduction of polymerization shrinkage stresses. The technique is, however, time-consuming and carries the risk of incorporating air bubbles or contaminants between incremental layers which can lead to strength reduction, inadequate marginal sealing, post-operative sensitivity and early restoration failure (McCabe & Ogden, 1987). To address the aforementioned lack, bulk-fill RBCs with lower polymerization shrinkage and depths of cure of up to 4 mm were developed by manufacturers (Benetti, Havndrup-Pedersen, Honore, Pedersen, & Pallesen, 2015; Czasch & Ilie, 2013; Ilie & Hickel, 2011; Jang, Park, & Hwang, 2015). The increased

depth of cure was achieved by improving material translucency by incorporating large size fillers and decreasing the filler load (Bucuta & Ilie, 2014; Ilie, Bucuta, & Draenert, 2013c; Lee, 2008). Some manufacturers added novel photo-initiators including germanium derivatives that substantially increase the absorption of visible light resulting in greater depth of cure (Moszner, Fischer, Ganster, Liska, & Rheinberger, 2008). Reduced photopolymerization time, lower water solubility, increased flexural strength and elastic modulus had also been reported with the use of novel photo-initiators (Moszner et al., 2008).

Efficient photopolymerization is essential to ensure the optimal clinical performance of RBCs and is influenced by intrinsic (material) and extrinsic factors including the type of light-curing unit (LCU) and curing light distance (Leprince, Palin, Hadis, Devaux, & Leloup, 2013). LCUs used in dentistry consist of quartz tungsten halogen (QTH) lamps, plasma arc curing (PAC) lights, argon-ion lasers (AL) and light-emitting diodes (LED). LED curing lights are most popular as they are lightweight, portable and highly effective. Polywave LED curing lights were introduced to achieve the wide spectral outputs of QTH lights catering to the extensive range of photoinitiators and RBCs available. Increasing the distance between the exit window of curing light guides and RBCs, intensifies light attenuation and decreases the power density (Meyer, Ernst, & Willershausen, 2002; Pires, Cvitko, Denehy, & Swift, 1993; Price, Derand, Sedarous, Andreou, & Loney, 2000) resulting in decreased surface hardness (SH) and degree of conversion (DC) (Price et al., 2000; Rode, Kawano, & Turbino, 2007; Vandewalle, Roberts, Andrus, & Dunn, 2005), hence, a decrease in the effectiveness of cure of RBCs.

Several studies have investigated the impact of curing light distance on conventional RBCs and reported decreased effectiveness of cure due to decreased SH with increasing distance (Rode et al., 2007; Thome, Steagall, Tachibana, Braga, & Turbino, 2007). In

addition, studies had also found a significant difference in the effectiveness of cure at the bottom surface of RBCs even at short curing light distances despite no substantial variation at the top surface (Aguiar, Lazzari, Lima, Ambrosano, & Lovadino, 2005; Pires et al., 1993).

Research pertaining to the effect of curing light distance on the cure of bulk-fill RBCs is still limited. The latter is clinically pertinent, considering the fact that bulk-fill RBCs are cured in 4 mm increments making the bottom surface of restorations particularly vulnerable to light attenuation as they are considerably further from the light source.

CHAPTER 2: AIM AND OBJECTIVES

2.1 Aim

To assess the effect of curing light distance on the effectiveness of cure of two different bulk-fill resin-based composites (RBC); Tetric N Ceram® Bulk Fill (TN) and Filtek™ Bulk Fill (FK).

2.2 Objectives

1. To determine the effect of curing light distance on the top and bottom surface hardness (SH) of bulk-fill RBC.
2. To examine the effectiveness of cure of bulk-fill RBC at different curing light distances.
3. To compare the effectiveness of cure between the bulk-fill RBC evaluated.

2.3 Null Hypothesis

1. The curing light distance has no influence on the SH of bulk-fill RBC.
2. The effectiveness of cure of bulk-fill RBC is not affected by different light-curing distances.
3. There is no difference between the effectiveness of cure of the evaluated bulk-fill RBCs.

CHAPTER 3: LITERATURE REVIEW

3.1 Resin-Based Composites (RBC)

A composite is a material which consists of at least two distinct phases, normally formed by blending components of different structures and properties (McCabe & Walls, 2008). RBC material is defined as "a highly cross-linked polymeric material reinforced by a dispersion of amorphous silica, glass, crystalline, or organic resin filler particles and/or short fibres bonded to the matrix by a coupling agent" ("The Glossary of Prosthodontic Terms: Ninth Edition," 2017). RBCs are used for a variety of applications in dentistry including but not limited to restorative materials, cavity liners, pit and fissure sealants, cores and build-ups, inlays, onlays, crowns, provisional restorations, cements for single or multiple tooth prostheses and for orthodontic devices, endodontic sealers, and root canal posts. It was first introduced in the 1950s (Ferracane, 2011) and has been continuously improved by the incorporation of different types and sizes of fillers, polymeric matrices and photoinitiators. RBC composition defines its chemical and physical properties depending on filler weight percent (wt.%) and volume percent (vol.%) which has led to different formulations tailored for their particular application.

Despite the different indications for RBCs, their main component comprises a blend of hard inorganic particles dispersed in a soft resin matrix. Generally, RBCs encompasses three main components; First is the resin matrix comprising a monomer system, an initiator system for free radical polymerization, and stabilizers. Second, the inorganic filler consisting of particles such as glass, quartz, and/or fused silica. Third is the coupling agent which is usually an organo-silane, that chemically bonds the reinforcing filler to the resin matrix, e.g., (methacryloxy)propyltrimethoxy silane (MPTMS) (Peutzfeldt, 1997).

3.1.1 Matrix of Resin-Based Composite

Dental resins are mainly based on methyl methacrylate monomers. In the late 1930s, poly (methyl methacrylate) was introduced to be used as denture base resin. A few years later, indirect filling resins were introduced which were then followed by direct resins. However, the methyl methacrylate resin was associated with significant defects, including large polymerization shrinkage, high coefficient of thermal expansion, severe discolouration, severe pulp damage, and high incidence of secondary caries (Peutzfeldt, 1997). Epoxy resins were then developed. This is a synthetic resin that could harden at room temperature with little shrinkage producing an insoluble polymer. It had better properties than methyl methacrylate resin. It was deemed to be a promising material used in the first dental RBC: an epoxy resin with aggregates of fused quartz or porcelain particles (Bowen, 1956). However, epoxy resins use was abandoned due to their slow hardening, preventing their use as a direct filling material.

In 1956, the era of dental RBCs started where Bowen synthesized a new monomer, 2,2-bis[4-(2-hydroxy-3-methacrylyloxypropoxy)phenyl]propane which is also known as Bis-GMA. It resembles an epoxy resin, however, the epoxy groups are replaced by methacrylate groups. It is prepared from bisphenol A and glycidyl methacrylate or diglycidyl ether of bisphenol A and methacrylic acid, therefore, it is a dimethacrylate (Bowen, 1959). Polymerization of the monomer occurs through the carbon-carbon double bonds (C=C) of the two methacrylate groups. Bis-GMA is superior to methyl methacrylate because of its large molecular size and chemical structure, providing lower volatility, lower polymerization shrinkage, more rapid hardening, and production of stronger and stiffer resins.

Due to the high viscosity of Bis-GMA, it is sometimes admixed with lower molecular weight dimethacrylates such as ethyleneglycol dimethacrylate (EGDMA), urethane

dimethacrylate (UDMA) or triethylene glycol dimethacrylate (TEGDMA) (Asmussen, 1975; Ruyter & Oysaed, 1987; Ruyter & Sjøvik, 1981; Vankerckhoven, Lambrechts, van Beylen, & Vanherle, 1981). This lower viscosity allows incorporating fillers in the material (Bowen, 1962 & 1963). The lower the viscosity of the monomer mixture, the more filler may be incorporated. It has been shown that the maximum polymerization rate of pure Bis-GMA occurs at less than 5% conversion due to its very high viscosity, and the final DC is limited to about 30%. In contrast, for pure TEGDMA, which is far less viscous, the maximum rate was observed at around 22% conversion, with a final DC of over 60%. Mixing the different co-monomers together resulted in intermediate values between these two extremes (Lovell, Newman, & Bowman, 1999).

While Bis-GMA is the most commonly used monomer in dental restorative materials, non-dimethacrylate monomers have been incorporated in some dental RBCs. Among these novel monomer technologies are those based on ring-opening epoxy chemistry (Filtek™ Silorane, 3M ESPE Dental Products, Seefeld, Germany). Additionally, a high-weight and low-viscosity monomer; Procrylat(2,2- bis-4-(3-hydroxy-propoxy-phenyl)propane dimethacrylate; was also introduced in some contemporary flowable RBCs e.g. Filtek™ Supreme XTE Flow (FS; 3M-ESPE, Seefeld, Germany). Procrylat resin is characterized by a lower viscosity and lack of pendant hydroxyl groups. However, contemporary dimethacrylate-based RBCs still represent the vast majority of commercially available materials for direct restoration (Leprince et al., 2013).

3.1.2 Fillers in Resin-Based Composite

The resinous matrix of dental RBC is incorporated with fillers that considerably influence the properties of the material. Fillers have several roles which include enhancing the modulus of elasticity, providing radiopacity, altering thermal expansion behaviour, and reducing polymerization shrinkage by reducing the resin fraction. Fillers

in RBC restorations can be classified as macrofillers, microfillers (pyrogenic silica) and microfiller-based complexes (Lutz & Phillips, 1983). Additionally, nanofillers are among the fillers that are incorporated in dental RBCs (Moszner & Klapdohr, 2004).

Macrofillers were the first to be used in dental RBCs. They are mechanically prepared from larger pieces of the material by grinding and/or crushing. The inorganic fillers are usually splinter shaped; and are made of quartz, glass, borosilicate, or a ceramic. Heavy metal glasses that provide adequate radiopacity are also available. Initially, the manufactured macrofillers size ranged between 0.1 and 100 μm with an average particle size between 5 to 30 μm. However, recent macrofillers size is ranging between 0.2 and 5 μm (Craig, 1981). Traditional or macrofilled RBCs allows the packing of the organic matrix providing higher inorganic filler loading. The use of these materials has been limited due to fillers dislodgement leaving a rough surface restoration (Lambrechts & Van Herle, 1982).

Microfillers were then introduced to produce different RBCs. Microfillers are derived chemically by hydrolysis and precipitation and consisting of finely dispersed radiolucent glass spheres. Originally, the primary particles commonly used had an average size of 0.04 μm. Recently, a tendency to use larger average particle sizes of approximately 0.05 to 0.1 μm is noticed (Lutz & Phillips, 1983). In an attempt to avoid the problems encountered with macrofilled RBCs, inorganic macrofillers and microfillers were combined to produce hybrid RBCs. They constitute a wide range of filler sizes within the range of 10-50 μm and 0.01-0.05 μm (Ferracane, 2011). The use of different filler sizes allowed intermediate aesthetic properties and good mechanical performance. It also led to efficient packing of the restoration and allowed the possibility of high filler loadings as high as 90 wt%. Acceptable surface smoothness can be achieved in these hybrid RBCs; however, wear pattern can result due to the presence of traditional macrofillers (Heuer,

Garman, Sherrer, & Williams, 1982). Therefore, homogenous microfilled RBCs were developed where the fillers are purely inorganic microfillers which are smaller than the wavelength of visible light. They have a high degree of surface polishability. Even though the microfillers can be dislodged because of wear, the polished surface retains its enamel-like lustre because the induced surface irregularities cannot be detected optically. Pyrogenic silica is an important representative of the microfillers used. It has a strong thickening effect if added directly to a liquid mixture. The viscosity of the material might be increased due to the large specific surface area of the microfillers. Therefore, alternative ways of admixing microfillers to an organic matrix were developed to increase the filler load without jeopardizing the handling properties (Lutz & Phillips, 1983).

Microfiller-based complexes were developed. They are divided into three different types depending on the manufacturing process: splintered prepolymerized microfilled complexes, spherical polymer-based microfilled complexes, and agglomerated microfiller complexes (Schmitt, Purrmann, Jochum, & Hubner, 1981). Splintered prepolymerized microfilled complexes are made by incorporating pyrogenic silica into a resin matrix and then heat-curing the mixture. After it sets, it is milled into particles with a size range between 1 and 200 μm. As for the spherical polymer-based microfilled complexes, they are manufactured by incorporating pyrogenic silica into partially cured polymer spheres that have an average diameter of 20 to 30 μm. These types of fillers are commonly named spherical prepolymerized particles. The final microfiller-based complex is the agglomerated microfiller one which consists of artificially agglomerated microfillers in the range between 1 and 25 μm. This type is purely inorganic unlike the above-mentioned types of complexes. Heterogenous microfilled RBC was developed where the filler content is admixed microfillers and microfiller-based complexes. These RBCs has increased filler loading, however, it resulted in an overall lower inorganic glass

content, around 50 wt % in comparison to traditional macrofilled RBCs (Anusavice, Shen, & Rawls, 2012).

Improvements in RBC technology have led to the introduction of new fillers with size ranging from around 5-100 nm (Moszner & Klapdohr, 2004). Nanofiller particles allow a homogeneous distribution in the resin matrix and led to a larger interface area between the fillers and resin matrix. It is predominantly made of crystalline silica and zirconia (Ilie, Rencz, & Hickel, 2013a). Nanofilled RBCs were introduced in the early 2000s. These contain discrete colloidal silica spherical nanoparticles or nanomers (5-100 nm). They also contain agglomerations of particles described as 'nanoclusters', in which the cluster size may be significantly above 100 nm, with a resulting improvement in filler loading (Cramer, Stansbury, & Bowman, 2011). The milling procedures are unable to reduce the filler particle size below 100 nm. Therefore, these nanoparticles are synthesized using synthetic chemical processes to produce building blocks on a molecular scale. These materials were then assembled into progressively larger structures and transformed into nanosized fillers suitable for a dental RBC (Mitra, Wu, & Holmes, 2003). The main advantages of nanofill RBCs are their superior resistance to wear (Yap, Tan, & Chung, 2004) and their high degree of polishability (Mitra et al., 2003). The nanoclusters provide a distinct reinforcing mechanism with enhanced entanglement between the nanofillers and the resin matrix compared with either microfill or hybrid systems, resulting in significant improvements in their strength and reliability (Beun, Glorieux, Devaux, Vreven, & Leloup, 2007; Curtis, Palin, Fleming, Shortall, & Marquis, 2009). Due to the high filler loading that can be obtained, polymerization shrinkage is also reduced (Moszner & Salz, 2001). The major drawback of nanofill composites is that they tend to be thick and sticky and to slump during clinical application (Al-Ahdal, Silikas, & Watts, 2014).

Nanohybrid RBCs were also introduced where they contain milled glass fillers of diameter within the range 0.6-3.0 μm. These RBCs are claimed to combine the wear characteristics provided by the small size of the particles in the agglomerated nanoclusters with the improved handling characteristics and aesthetics of the microhybrid RBCs. However, a study assessing a number of commercially available materials marketed as 'nanohybrids' in comparison to nanofilled and microhybrid materials has shown that nanohybrid materials exhibited inferior diametral tensile strength compared to nanofilled and microhybrid RBCs, and similar or slightly better wear resistance compared to microhybrids in terms of retention of surface smoothness (de Moraes et al., 2009).

RBC classification based on filler size such as the macrofilled, microfilled, and hybrid materials has shown useful correlation with the aesthetic, surface, and mechanical performance with early types of RBC. However, the usefulness of this classification may be compromised nowadays since most current composites are either microhybrids or nanohybrids. Also, there is an increasing diversity of filler shapes, materials, distribution, and organic matrix components of current RBC which may affect the performance of the materials; thus, the final properties are being more material-dependent than being dependent on filler size classification alone.

3.1.3 Additives in Resin-Based Composite

In general, dental RBCs contain a mixture of at least two different fillers. A number of additives are further incorporated within the material. Some elements such as Yttrium fluoride (YbF_3) which serves as a radioopacifier, fluorosilicate glasses, or sparing amounts of soluble fluoride salts are added to the RBCs. Inhibitors such as phenols, e.g. 2,6-di-tert-butyl-methylphenol (BHT) and hydroquinone monomethylether (MEHQ), are also added to the resin formulation. Their amounts range between 200 and 1000 ppm preventing premature polymerization during the storage of the RBC and avoiding

uncontrolled photopolymerization by normal room light during their use. Ultraviolet (UV) photostabilizers such as 2-hydroxybenzophenones or 3-(2-hydroxyphenyl)-benzotriazoles are also added to protect the RBCs against photodegradation of the organic matrix which may cause colour changes of the material. Finally, colour pigments are added in order to meet the aesthetic demands by incorporating a mixture of different inorganic pigments (yellow, red, white, and black) to imitate the colour of the natural teeth (Klapdohr & Moszner, 2004).

3.2 Polymerization of Resin-Based Composites

Early RBCs were supplied as power/liquid, self-curing direct, acrylic-based restorative materials. Dual-paste, self-cure RBC systems were then introduced and eventually the light-cured single paste system was developed (Craig, 1981). This continuous development was the result of attempts to improve the materials' properties. Nowadays, light-activated RBCs are predominantly used, some of which might be dual-cured containing a chemically cured component. Photopolymerization is defined as "a chemical reaction wherein photons activate an initiator which will react in the presence of an aliphatic amine with the urethane dimethacrylate oligomer and an acrylic copolymer" ("The Glossary of Prosthodontic Terms: Ninth Edition," 2017). In other words, photopolymerization is the conversion of monomers into polymers when RBC material is exposed to light. This process usually starts at the surface where light is applied leading to a rapid increase in the DC and crosslinking density.

3.2.1 Kinetics of Photopolymerization Reaction

Previous studies have been carried out to describe the kinetic behaviour of photopolymerization and to clarify the onset of RBC network formation. Generally, photopolymerization is divided into three main steps. The first is the initiation process

which is characterized by free radical formation leading to the start of the reaction. Second is the propagation process where chain growth takes place. This stage is further subdivided into: the quasistatic process where the number of high molecular weight chains increases resulting in viscosity increases; the gel phase or the Trommsdorff-Norrish effect (Dionisio, Mahabadi, O'Driscoll, Abuin, & Lissi, 1979) where the reaction rate increases and viscosity is further increased due to the slow termination reactions; and finally, the glass phase which is a gelatinous phase and is accompanied by a decrease in the reaction rate. The third step of the photopolymerization process is the termination which occurs when two free radicals join, or when one molecule abstracts a hydrogen atom from another, forming a C=C.

During the photopolymerization of the dental RBCs, the DC and the crosslinking density increase rapidly. This results in a rapid increase in viscosity that reaches the gelation state, where the polymer matrix becomes rigid. Both propagation and termination reactions are diffusion-controlled (Anseth, Wang, & Bowman, 1994). The propagation process involves the reaction of polymeric radical and methacrylate monomer. This does not become diffusion-controlled until the polymer reaches the glassy phase in a process known as ‘vitrification’. As the polymer vitrifies, the propagation reaction slows and the polymerization ceases, i.e., auto-deceleration occurs. This process is particularly important in dental RBCs, where auto-deceleration results in residual, unreacted methacrylates that remain in the RBC restoration. In contrast to the propagation reaction, in the termination reaction, the radical concentration and polymerization rate increases significantly, a phenomenon referred to as ‘auto-acceleration’. This process is important for dental RBCs since it results in rapid photopolymerization within a clinically acceptable time.

In addition to the complex polymerization kinetics, the polymer structure also evolves with numerous complexities. Two critical macroscopic demarcations occur during polymerization. The first is the gel point conversion which represents the point at which an infinitely cross-linked polymer network first appears, accompanied by an increase in viscosity and poorer flow (Leprince et al., 2013). The DC of dimethacrylates at the gel point is expected to be less than 1-5% (Stansbury et al., 2005). The second macroscale demarcation is the vitrification point, which represents the conversion at which the polymer becomes glassy, accompanied by a significant increase in modulus and viscosity. When the vitrification point is reached, the reactive dimethacrylate groups become increasingly less able to migrate to the reaction sites than in the gel stage.

It should be noted that polymer networks are extremely heterogeneous due to two main facts. The first is due to the formation of microgels near the initiation sites and the second is due to the presence of pendant methacrylate groups in Bis-GMA, TEGDMA monomers or other analogous systems which might be more reactive than their monomeric counterparts (Elliott, Lovell, & Bowman, 2001). A pendant is a small chain that hangs off of the main chain which is the backbone of the polymer. This heterogenicity has significant implications on RBC restorations affecting its post-cure behaviour (Truffier-Boutry et al., 2006) and the refractive index variation within the polymer matrix enhancing the RBC translucency (Howard, Wilson, Newman, Pfeifer, & Stansbury, 2010).

3.2.2 Oxygen Inhibiting Layer

The polymerization reaction of dental RBCs is based on the presence of free radicals that induces the reaction. Oxygen is considered as a free-radical scavenger (Xia & Cook, 2003). It diffuses from the atmosphere into RBCs causing the oxidation of radicals into stable species known as hydroperoxides (Andrzejewska, Lindén, & Rabek, 1998; Schulze

& Vogel, 1998) which have low reactivity toward monomers. If the concentration of these hydroperoxides is sufficient, they can alter the properties of the polymer. Diffusion of oxygen into the exposed resin or RBC surface, as polymerization proceeds, results in quenching of both initiator and polymer-based radical species and is responsible for the poorly polymerized, air-inhibited surface layer (Finger, Lee, & Podszun, 1996). The inhibitory effect of oxygen was found to affect resin polymerization to a depth of 53 µm (Rueggeberg & Margeson, 1990).

3.2.3 Post-Polymerization Reaction

After the photocuring of RBCs, it has been observed that the polymerization reaction is not complete. An additional cure was reported to range between 5 minutes and 24 hours representing 19-26% of the final DC depending upon the material (Halvorson, Erickson, & Davidson, 2002). However, another study noted that DC had a very minimal increase of more or less 2% during the first 24 hours which was not considered a significant increase (Truffier-Boutry et al., 2006). Extrapolating these findings clinically, it was found that small amounts of unreacted monomers from polymerized material are eluted (Lagocka et al., 2018) into either the oral cavity or through dentinal diffusion (Gerzina & Hume, 1996) into the pulpal tissues, hence leaching into the blood circulation (Bouillaguet, Wataha, Hanks, Ciucchi, & Holz, 1996). Unreacted monomers from dental RBCs were found to be cytotoxic (Lee, Kim, Kwon, Lee, & Kim, 2017) and might cause local adverse effects (Nocca et al., 2007). However, not all residual monomers are eluted into an aqueous solution (Ferracane, 1994). Pulp studies have shown a lack of significant pulpal irritation after the placement of properly sealed RBC restorations (Cox, Keall, Keall, Ostro, & Bergenholtz, 1987). It was reported that 75% of the elutable molecules are extracted within a few hours and that 95% are extracted within 24 hours (Ferracane & Condon, 1990). Therefore, RBCs do not provide a chronic source of unreacted monomer to the pulp or other oral tissues (Ferracane & Condon, 1990). However, the

unreacted monomers and/or functional groups within the polymer can act as plasticizers and therefore, might have a negative impact on the mechanical properties due to the lower cross-linking of the polymer resulting in lower DC (Durner, Obermaier, Draenert, & Ilie, 2012).

3.3 Photoinitiators

A photoinitiator is a molecule that can absorb light and, as a result, either directly or indirectly, generate reactive radicals that can initiate polymerization (Fouassier, 1995). Hence, the photoinitiator is a compound that can transform the physical energy of light into suitable chemical energy in the form of reactive intermediates. Photoinitiators can be classified into Norrish Type I and II initiators. Norrish Type I initiators are typically compounds containing benzoyl groups which undergo cleavage when exposed to visible light to generate two free radicals where at least one the free radicals react with monomers to initiate polymerization. They do not require a co-initiator to produce free radicals. However, Norrish Type II initiators absorb visible light to form excited molecules which abstract a hydrogen atom from a donor molecule (synergist). The donor then reacts with a monomer to initiate polymerization. Photoinitiators are incorporated in dental RBC to start the polymerization reaction.

3.3.1 Camphorquinone (CQ)

CQ (1,7,7-trimethylbicyclo[2.2.1] heptane-2,3-dione) Type II initiator system is the most widely used photoinitiator in dental RBCs (Stansbury, 2000). It is a diketone molecule that creates free radicals to initiate the photopolymerization process. A co-initiator is required for an efficient polymerization process to occur. In case of dental RBC restorative containing CQ, tertiary amine photoreductant is the co-initiator. Both the

CQ and the tertiary amine molecule react together to provide reactive radicals that begin polymerization of the methacrylate resin system.

CQ molecule has two carbonyl groups in its structure. Homolytic cleavage of the C=C in these two carbonyl groups results in the formation of two carbonyl radicals. These radicals escape forming photo-decomposed products, which results in a decrease in the concentration of the active CQ molecules. These pair of radicals remain structurally connected to each other and might recombine again to reform the CQ molecules. Recombination can be greatly reduced by the addition of aliphatic or aromatic amine co-initiators, which may also serve to increase the rate of photodecomposition and polymerization efficiencies (Sun & Chae, 2000).

The maximum absorbance peak of CQ is at 468 nm, but it could be activated in a range between 400 and 500 nm (Neumann, Schmitt, Ferreira, & Correa, 2006). It was also found to be activated by the LCUs of wavelengths below 320 nm (Jakubiak et al., 2003).

3.3.2 Recent Photoinitiators

CQ colour is intense yellow (Janda, Roulet, Kaminsky, Steffin, & Latta, 2004) and only a portion of CQ is utilized during photopolymerization (Jakubiak, Sionkowska, Lindén, & Rabek, 2001). Therefore, alternative lighter-coloured initiators that completely bleach out after photopolymerization have been recently used. These include acyl phosphine oxide (APO), phenyl propanedione (PPD), and Ivocerin®. All these photoinitiators have different spectral absorbance ranges of activity, and also differ greatly in their ability to absorb light (Neumann et al., 2006).

3.3.2.1 Acyl Phosphine Oxide (APO)

APO is a Type I initiator that has high absorbency and efficient quantum yields (Neumann et al., 2006). The sensitivity peak of APO is approximately 370 nm, which is

considerably lower than that of CQ. Two variations of APO initiators are used in dental restorative materials: monoacylphosphine oxide (MAPO) and bisacylphosphine oxide (BAPO). Lucirin® TPO (2,4,6-trimethylbenzoyldiphenylphosphine oxide) is a representative of MAPO initiator. The absorption spectrum of TPO is seen mainly in the UV range. It was incorporated in the dental RBC as the sole initiator, but currently, TPO is combined with CQ (and other photoinitiators) to provide enhanced resin photopolymerization and decrease the yellowing of the restoration (de Oliveira et al., 2016; Leprince et al., 2011). Irgacure 819, is a representative of BAPO. It was found to be very sensitive to light below 440 nm (Neumann et al., 2006).

3.3.2.2 Phenyl Propanedione (PPD)

Phenyl propanedione (1-phenyl-1,2-propanedione) is another Type II initiator that has more broad-banded absorption spectrum which extends from the UV wavelength range to approximately 490 nm. It is usually combined with CQ resulting in a synergistic effect, leading to enhanced resin polymerization and also slowing the overall rate of the reaction. It also contributes to the reduction of the residual yellow colour of the restorative material (Schneider, Cavalcante, Consani, & Ferracane, 2009).

3.3.2.3 Ivocerin®

Ivocerin® is a new germanium-based photoinitiator that is patented by one manufacturer (Ivoclar Vivadent, Schaan, Liechtenstein). It has a broader spectrum and absorbs light at a higher wavelength range than APO and has a sensitivity peak of about 420 nm. It is characterized by high quantum efficiency, high absorption capacity and very good bleaching properties. It is claimed to produce highly reactive polymerization in very small amounts, therefore, it is considered as a polymerization booster.

3.4 Bulk-Fill Resin-Based Composites

Polymerization shrinkage is considered as the most significant problem with current RBC restorations. It is an intrinsic property of conventional resin-based materials caused by the approximation of monomers during polymerization, i.e. the distance between monomers is reduced due to the conversion of the weak van der Waals forces into covalent bonds. Polymerization shrinkage is a primary contributor to premature failure due to its contribution to internal and marginal gaps, microleakage, and micro-cracking of tooth structure due to cuspal deflection (Ferracane & Mitchem, 2003; Goncalves, Azevedo, Ferracane, & Braga, 2011). Polymerization stress occurs in most of the clinically relevant cavity configurations and is dictated by multiple factors including resin viscosity, volume shrinkage, polymerization rate, DC, modulus development and network structural evolution. The C-factor is among the determinants of polymerization shrinkage. It is defined as the ratio of bonded to the unbonded surface area of the restoration. The degree of resin flow is determined by the material and the C-factor (Davidson, 1986). An increased rate of shrinkage stress development with a high C-factor leads to a decrease in flow capacity which is not sufficient to preserve adhesion to dentine by dentine bonding agents (Feilzer et al., 1987).

3.4.1 Techniques for Resin-Based Composite Application

3.4.1.1 Incremental Technique

Multiple studies were carried out to determine how to reduce the overall polymerization shrinkage and internal stresses to decrease the clinical issues of RBC restorations. Insertion of RBC in increments of 2 mm or less was among the proposed techniques to reduce the overall volume of the resin and therefore, the polymerization shrinkage. This was shown to reduce the stresses generated at the cavity walls (Lutz, Krejci, & Barbakow, 1991).

Several techniques were suggested for the application of these 2 mm increments to lower the C-factor, such as horizontal incremental, oblique incremental (Lutz, Krejci, & Oldenburg, 1986), centripetal incremental (Bichacho, 1994) and split horizontal incremental techniques (Hassan & Khier, 2005). However, these techniques are time-consuming, where each layer has to be incorporated in a certain way and photopolymerized before proceeding to the following layer. This has led to more time spent to complete the chairside procedure. Another problem encountered was the presence of air bubbles incorporated between layers. These porosities enhance the propagation of cracks within the resin, reducing the fatigue strength and increasing the wear rate of the material (McCabe & Ogden, 1987). The incorporation of air into the resin matrix may, therefore, be detrimental to the durability of the material and the need to avoid procedures or reduce the number of procedures that are likely to influence the levels of porosity within the material.

3.4.1.2 Bulk-Fill Technique

In an attempt to solve the shortcomings of conventional RBCs, bulk-fill materials were introduced where they could be applied in 4-5 mm layers according to the manufacturer instruction (Ilie & Hickel, 2011). Although they are advertised as a new material category, they do not essentially differ in their chemical composition from regular microhybrid and nanohybrid RBCs. The matrix resin is mainly based on monomers of Bis-GMA, UDMA, TEGDMA, and EBPDMA. However, some bulk-fill RBCs have modified Bis-GMA resulting in a monomer of lower viscosity. The fillers in bulk-fill RBCs are lower in filling percentage by volume, but higher by weight in comparison to conventional microhybrid and nanohybrid RBCs, in other words, bulk-fill RBCs contain a lower filler content and an enlarged filler size.

3.4.2 Bulk-Fill Resin-Based Composites in the Dental Market

In 2009, the first bulk-fill RBC (Surefil SDR® flow, Dentsply) was introduced in the market with flowable consistency. It was indicated for use as a base in Class I and Class II cavity preparations, requiring an additional layer of 2 mm of conventional RBC on the occlusal surface. The manufacturer patented stress decreasing resin (SDR) technology which allows greater molecule flexibility thus, avoiding the stress generated during photocuring (Dentsply, 2011; Ilie & Hickel, 2011).

Later, bulk-fill RBCs with similar consistency and application methods appeared in the market (x-tra base, VOCO; Filtek™ BulkFill Flowable, 3M ESPE and Venus® BulkFill, Heraeus Kulzer). For Filtek™ BulkFill Flowable (3M ESPE), the manufacturer claims that it is based on four monomers: BisGMA, UDMA, Procrylat, and BisEMA, which have high molecular weight, to reduce the development of polymerization shrinkage. Procrylat monomer is added to allow greater fluidity and thus lowering the polymerization stress (Ilie & Hickel, 2011).

For all the above RBCs, the manufacturers have not announced major changes to the polymerization system. Subsequently, a different bulk-fill RBC variation (Tetric N Ceram® Bulk Fill, Ivoclar Vivadent and x-tra fil, VOCO) was introduced which had conventional consistency and indicated to be used in increments of up to 4 mm without the need for an extra occlusal layer. In the case of flowable bulk-fill RBCs, the inorganic filler ranges between 64-75 wt.% and 38-61 vol.%. On the other hand, in most of the high-viscosity bulk-fill RBCs, this component was increased up to 79-86 wt.% and 61-81 vol.%.

Tetric N Ceram® Bulk Fill (Ivoclar Vivadent) has a new polymerization initiation booster called Ivocerin®, which is a germanium based photoinitiator of greater reactivity than that of CQ, due to its higher absorption of visible light (400 to 450 nm) (Moszner et

al., 2008). It was also reported that it has a filter for light pollution that ensures proper clinical work time.

A third variation of bulk-fill was introduced (SonicFill™, Kerr) which depends on special sonic vibration handpiece and it is used in 5 mm increments. It is activated by means of sound vibration, producing a momentary drop in viscosity during application. This resin is also indicated for Class I and II preparations with no occlusal layer.

3.4.3 Properties of Bulk-Fill Composites

Generally, bulk-fill RBCs have a lower proportion of fillers with an increase in their size which was claimed to decrease problems encountered with conventional RBCs. Multiple *in vitro* studies evaluated different properties for the newly introduced bulk-fill RBCs. One of the main concerns was the depth of cure of 4 mm increment which was recommended by the manufacturers. In conventional photopolymerized RBCs, limited curing depth was found and the possibility of insufficient monomer conversion in the bottom of the cavity preparation was speculated (Lindberg, Peutzfeldt, & van Dijken, 2005). Some studies found an improved depth of cure of bulk-fill RBCs in comparison to conventional ones, while others found no improvement. Several reasons have been proposed to explain the improved depth of cure. The first suggested reason was the inclusion of more efficient initiation systems in some resins which was claimed to improve the light penetration in the RBC (Alrahlah, Silikas, & Watts, 2014). A second suggested reason is that bulk-fill RBCs have higher translucency which would allow deeper light penetration (Bucuta & Ilie, 2014). Another reason is that decreased matrix-filler surface interface, which reduces light refraction and improves light penetration (Ilie et al., 2013c). Reduction in refractive index differences between resin and filler improved the DC (Fujita, Nishiyama, Nemoto, Okada, & Ikemi, 2005), and increased depth of cure as well as colour shade matching (Shortall, Palin, & Burtscher, 2008).

3.4.3.1 Polymerization Shrinkage and Stress

It was found that some bulk-fill flowable RBCs were effectively cured in 4 mm bulk, but shrank more than the conventional non-flowable RBCs. (Jang et al., 2015). However, bulk-fill non-flowable RBC showed comparable shrinkage to conventional non-flowable RBC, but it was not sufficiently cured in 4 mm bulk (Jang et al., 2015). When evaluating the polymerization stress of bulk-fill RBCs, it was found to be lower than conventional RBCs and conventional flowable RBCs (El-Damanhoury & Platt, 2014; Ilie & Hickel, 2011). However, in another study, it was found that polymerization shrinkage of bulk-fill RBCs might be smaller, similar or larger than conventional flowable RBCs (Garcia, Yaman, Dennison, & Neiva, 2014). This has shown the relationship between the proportion of filler and polymerization shrinkage, where the resins with the least amount of filler loading, and therefore with the greater proportion of resinous matrix, experienced higher levels of shrinkage by polymerization, and vice versa.

3.4.3.2 Cuspal Flexure

Cuspal flexure was evaluated in premolars with Class II restorations restored with bulk-fill RBCs applied in one increment, it was significantly lower than those observed in conventional RBCs applied in incremental layers (Moorthy et al., 2012). However, it is difficult to determine if the lower cusp flexure observed by using bulk-fill RBC was due to a smaller contraction of the resin or due to changes in the mode of application of the material. A study has determined the existence of a smaller change in the inter-cusp distance when RBC was placed as a single increment in comparison to the incremental method. It was reasoned that each increment would cause deformation of the cavity's walls with the downward movement of the walls and towards the inside. This movement decreases the total volume of the cavity. In contrast, RBC placed using single increment technique the cavity volume remains relatively the same (Versluis, Douglas, Cross, & Sakaguchi, 1996).

3.4.3.3 Marginal Adaptability

RBC marginal adaptability is closely related to the development of polymerization shrinkage and stress. Studies found no significant differences in marginal integrity when using bulk-fill RBCs in comparison to conventional RBCs (Roggendorf, Kramer, Appelt, Naumann, & Frankenberger, 2011). Several studies evaluated the viscosity of bulk-fill RBCs in relation to different properties. It was found that the use of flowable RBC results in better adaptation compared to packable RBCs (Opdam, Roeters, Joosten, & Veeke, 2002).

3.5 Light Curing Units

A diversity of dental light-curing units are available in the market. These include Quartz-tungsten-halogen lights (QTH), plasma-arc lights (PAC), argon-ion lasers (AL) and Light-emitting diodes (LED).

3.5.1 Quartz-Tungsten-Halogen Light (QTH)

QTH was the first visible light used to cure RBCs. Its bulb consists of a tungsten filament enclosed in a clear, crystalline quartz casing, filled with a halogen-based gas. As electricity flows through the filament, heat develops because of the wire resistance. The heat developed is sufficient to cause tungsten atoms to vaporize from the wire surface. When this happens, tremendous amounts of electromagnetic energy are released, mostly occurring in the infrared (IR) spectral region. Thus, these types of light units typically require filtering to remove heat, as well as excess visible light not required for photopolymerization.

3.5.2 Plasma-Arc Light (PAC)

PAC was introduced to photopolymerize RBCs. These units utilize two tungsten rods, held at a specified distance, encased in a high-pressure envelope of xenon gas, with a sapphire window through which emitted radiation escapes. When a high voltage is applied across the electrodes, a spark forms, which produces a tremendous amount of electromagnetic radiation over a wide spectral range: from IR to short wavelength UV. Because of the massive amount of radiation emitted falling outside of the narrow limits needed for dental photopolymerization, a substantial amount of filtering is required in this light. Additionally, there is a special liquid that helps to further reduce unwanted IR, UV, and visible light (Rueggeberg, 2011).

3.5.3 Argon-Ion Laser

Argon-ion laser was used to enhance vital tooth bleaching before being used for intraoral photopolymerization of dental RBCs. The initial delivery of power from the laser to the tooth was directly through the end of a fibre optic cable. The radiation coming out of the fibre optic cable had a divergent nature, and therefore, other methods were developed in an attempt to make a collimated beam of coherent energy, whose target power was not related to the curing light guide-to-tooth distance. However, these units were large, heavy, and expensive. Over time, the unit became much smaller, and could easily fit into a clinic, yet, it needed to be on a cart when moved from room-to-room due to its weight. Additionally, after the use of the device, room temperature would be elevated. Due to the above reasons, this curing system became outdated in a short time (Rueggeberg, 2011).

3.5.4 Light Emitting Diodes (LED)

The LED technology has been proven to be an efficient, cost-effective lighting source. It has been widely used shortly after the blue LEDs became available using indium-

gallium-nitride (InGaN) substrates (Rueggeberg, 1999). These devices rely on the forward-biased energy difference (band gap) between two dissimilar semiconductor substrates (n-type conduction band, and p-type valence band), to determine the wavelength of emitted light (Rueggeberg, 1999). Electrons are forced to traverse from one side of a semiconductor material (the "N" material, having an excess of electrons) to a substrate having an electron deficiency (the "P" material). When electrons travel through this potential energy "gap", they emit light with wavelength depending on the composition of each semiconductor substrate. The spectral emission from such units could successfully photo-activate CQ-based products.

3.5.5 Development in Light Emitting Diodes

Light-emitting diodes (LED) technology was borrowed from other industries and was incorporated in the dental field in the 1990s. The concept that the spectral emission from such units could successfully photo-activate CQ-based products has been proven. The LED technology requires low power, no filament, no optical filter and therefore provides much greater photon-generating efficiency than any competitive light source. In addition, these units can be powered by a battery. The LED sources are claimed to last for thousands of hours without needing replacement (Rueggeberg, 1999).

LED technology depends on indium-gallium-nitride (InGaN) substrates. In a typical circuit, electrons are forced to traverse from one side of a semiconductor material (the "N" material, having an excess of electrons) to a substrate having an electron deficiency (the "P" material). When electrons travel through this potential energy "gap", they also emit light, the specific wavelength of which is determined by the composition of each semiconductor substrate.

3.5.5.1 First Generation

These were the first introduced blue LED curing lights and were mainly experimental. They were built to test whether they could generate light at the correct wavelength and deliver a sufficient number of photons needed to successfully photopolymerize dental RBCs. The individual LED available at that time had a very low output power which necessitated the different arrangement of multiple LED elements into a physical array, and a turbo-tip was used resulting in a sufficient output which was enough for photopolymerization of CQ-based RBCs.

These closely packed arrays generated a significant amount of thermal energy, and therefore, heat dissipation was needed. Heat sinking technology was incorporated in some units to draw heat away from the LED chip. Other units have used metal body castings that provided a large area for the thermal dissipation as well as structural durability.

The first generation LED did not produce adequate output for curing RBCs resulting in insufficient depths of cure of dental RBCs (Ernst et al., 2004). However, if the curing unit was used for extended exposures, their output was found to be comparable with QTH source (Ernst et al., 2004). The irradiance value of this LED generation varied greatly between different units. Nickel-cadmium (NiCAD) battery was used, but careful recharging routines had to be followed or the useful lifetime of these power sources was significantly reduced. The spectral emission of this light was effective for activation of CQ and PPD, but it was not suitable with TPO (Rueggeberg, 1999).

3.5.5.2 Second Generation

In the illumination industry, high emission area LEDs became available and were adapted in dentistry. One-Watt chips were available, all on one body, consisting of four main areas of illumination, each consisting of four, bar-shaped emitting surfaces: a total of sixteen emission areas. Incorporation of these chip types greatly boosted irradiant

output and allowed blue LEDs to be able to accomplish effective photopolymerization in a much shorter time. A higher-power LED became available shortly thereafter containing five-Watt devices and rapid advances have led to chips reaching 10 and 15 Watts which were incorporated in dental LEDs. These resulted in a greater photon density increasing irradiance values and allowed lower exposure time to achieve optimal photopolymerization of CQ-containing restorative materials (Uhl, Sigusch, & Jandt, 2004).

Concurrently, battery technology also advanced, allowing incorporation of the longer-lasting nickel-metal hydride (NiMH) units. Higher-rated LED chips produced a lot of heat and therefore advanced methods such as internal fans and large metal heat sinks were used to dissipate thermal power from the LED arrays (Rueggeberg, 1999).

As for the emission spectra of this generation, it is much greater than the first one. However, the peak emission is located at a shorter wavelength than previously seen leading to an increased overlap with PPD while still providing activation of CQ. No interaction with APO was possible.

3.5.5.3 Third Generation

The need to provide radiant energy to activate TPO as well as Ivocerin® drove manufacturers to incorporate more than one colour into the LED chipset. These LCUs are known as polywave as they emit irradiation with different peaks of wavelengths. Different arrays were used to provide a simultaneous combination of violet and blue wavelengths. Among the chip arrangements was an array with centrally positioned, high-wattage blue LED, surrounded by four lower-powered, converging violet LEDs. Another array incorporated two blue LEDs and one violet LED. This array arrangement is seen in Bluephase Style light. A third array was the arrangement of three different colour chips

into the single array set: two blue (emitting near 460 nm), a shorter wavelength blue (emitting near 445 nm), and one violet, emitting close to 400 nm).

With the inclusion of the violet emission near 407 nm, photons are delivered to a wide bandwidth for all photoinitiators used in dental restorative materials, particularly for TPO, PPD, and CQ. However, in the third generation, the blue emission is reduced compared to that of an all-blue emitting light, which means less potential for CQ activation at RBC depths. In materials that contain Lucirin® TPO or Ivocerin® in addition to CQ, improved curing is possible, even with the lower blue light present. Despite the differences in the amount of violet and blue light emitted by the polywave LED, previous evidence supports the idea that the spectral output of this polywave LED used was enough to efficiently cure bulk-fill RBCs containing either CQ or CQ associated with alternative photoinitiators (Schneider, Pfeifer, Consani, Prahl, & Ferracane, 2008). However, the light beam profile received by the specimen should not be ignored.

The third generation curing lights are present in two different designs. The first is the traditional guns style light which has the chipset inside the gun body and uses fibre optic light guides to transmit emitter photons onto the target area. Another concept is the use of a pencil-style body which can still use removable fibre optic guides or can have the emitting chipset placed directly at the distal guide end of the unit. This allows the light to directly shine onto the target, without the use of fibre optic light guides. It also has the advantage of greater ease of placement intraorally facilitating light guide position and allowing more direct illumination and maximum transfer of light to the restoration. Battery technology has been advanced and the use of lithium-ion batteries is common in most of the LED units of this generation. They are stable and durable allowing long-usage energy storage sources providing a reliable output over extended clinical operation time.

3.6 Effectiveness of Cure of Resin-Based Composite

Effectiveness of cure of RBCs is a crucial parameter that evaluates the extent of material polymerization. An RBC that is cured effectively ensures optimum clinical performance due to an acceptable DC of monomers into polymers which results in enhanced mechanical properties of the material. The effectiveness of RBC cure may be assessed directly or indirectly. Direct methods using vibrational spectroscopy such as IR spectroscopy and laser Raman spectroscopy assess DC. However, indirect methods include ISO 4049 method and SH testing.

3.6.1 Vibrational Spectroscopy

These methods provide a direct approach to determine the effectiveness of cure by measuring the DC (Asmussen, 1982b; Eliades, Vougiouklakis, & Caputo, 1987; Ferracane & Greener, 1984; Rueggeberg & Craig, 1988). This is achieved by measuring both the percentage of carbon-carbon single bonds in the cured material and the percentage of unreacted C=C bonds. Vibrational spectroscopy can be classified into two techniques. The first technique is Fourier Transform Infrared Spectroscopy (FTIR) which is sometimes documented as IR Spectroscopy and is based on light absorption. The second technique, Raman Spectroscopy is based on light scattering. There are two devices which are popularly used; Fourier Transform-Raman Spectroscopy (FT-Raman) and micro-Raman Spectroscopy (MRS) (De Santis & Baldi, 2004). Other available techniques include differential thermal analysis (DTA), differential scanning calorimetry (DSC) and nuclear magnetic resonance (NMR) (Alshihri, Santini, & Aldossary, 2018).

3.6.2 ISO 4049 Method

It is a method primarily for manufacturers to certify that their RBCs will achieve the minimal depth of cure requirement. They also provide recommendations for light-curing times relative to RBC increment thickness to adequately polymerize the material. Some

studies have also used this method to determine the effectiveness of cure of the tested RBC (Ruyter & Oysaed, 1982). Samples are prepared in a cylindrical stainless-steel mould of dimensions 6 mm long x 4 mm diameter. If the manufacturer claims a depth of cure of 3 mm, the mould should be at least 2 mm longer than twice the claimed depth of cure. After polymerization of the specimen, it should be removed from the mould and scraping of uncured material is done with a plastic instrument. A micrometre is used to measure the height of the cured material, where the values are divided by 2 to give the depth of cure of the tested RBC (ISO_4049, 2009). According to ISO 4049-2009, the depth of cure should be no more than 0.5 mm below the value stated by the manufacturer.

The rationale behind ISO 4049 is unspecified and the correlations between the test and clinical performance are lacking. It was concluded that the ISO 4049 method overestimated the depth of cure when it was compared with Knoop hardness profiles (Moore, Platt, Borges, Chu, & Katsilieri, 2008) and Vickers hardness estimations of the DC (Flury, Hayoz, Peutzfeldt, Husler, & Lussi, 2012).

3.6.3 Surface Hardness (SH)

SH is a well-accepted method and has been used to indirectly probe polymer network conversion therefore, hardness profiles can be used to measure the depth of cure. Ideally, SH of RBC should be equal or close to equal throughout the restoration and for the life of the restoration. However, the SH of bulk-fill RBC has different values at different depths (Garcia et al., 2014). Therefore, sufficient cure was defined as SH of more than 80% between the bottom to top surfaces (B/T ratio) of RBC samples (Johnston, Leung, & Fan, 1985).

As a measure of the completeness of conversion, the bottom to top Knoop hardness number (B/T-KHN) was approximately 2.5 times more sensitive than the bottom to top DC (B/T-DC) ratio (Bouschlicher, Rueggeberg, & Wilson, 2004). B/T-KHN ratios

provide an accurate, simple method of assessing the efficacy of photoinitiation strategies (curing light/exposure duration) instead of using more complex FTIR methods to determine the DC (Bouschlicher et al., 2004).

3.7 The influence of Curing Light Distance on the Effectiveness of Cure of Resin-Based Composites

Among the factors that affect the effectiveness of cure of RBCs is the distance between the surface of the restoration and the LCU guide. Manufacturers recommend positioning the curing light guide as close as possible to the RBC restoration surface. These recommendations are typically based on testing the material in ideal laboratory conditions, commonly at a curing light distance of 0 mm (Shortall, Price, MacKenzie, & Burke, 2016). However, in a clinical setting, this curing light distance is difficult to achieve especially in Class II cavities. One study measured the depths of Class II proximal cavities of 1146 extracted teeth. They reported an average depth of 4-5 mm for mandibular premolars, 5-6 mm for maxillary premolars and 5-7 mm for molars (Hansen & Asmussen, 1997). This was in agreement with another study that found that 6.3 mm (± 0.7 mm) was the typical Class II cavity depth when the LCU guide was positioned directly on the tooth or the restoration surface (Price et al., 2000). Additionally, more than 15% of the mandibular molars were reported to have a proximal cavity depth of more than 8 mm (Hansen & Asmussen, 1997).

Several studies have investigated the impact of curing light distance on the effectiveness of cure of conventional RBCs. Most of these studies found that the SH of the RBC decreases with increasing the curing light distance (Caldas, de Almeida, Correr-Sobrinho, Sinhoreti, & Consani, 2003; Rode et al., 2007; Thome et al., 2007). Other studies found that there was no statistical difference of the top SH of RBCs at small curing

light distances, however, the bottom SH was statistically significant at the same small curing light distances (Aguiar et al., 2005; Pires et al., 1993). Up to date, most of the studies assessing the effectiveness of cure of RBCs at different curing light distances were done on conventional RBCs, however, scarce studies were done on bulk-fill RBCs.

CHAPTER 4: MATERIALS AND METHODOLOGY

In this *in vitro* study, two packable bulk-fill RBCs of different compositions were cured with a polywave LCU at different curing light distances. RBC samples were prepared and stored for 24 hours. The Knoop hardness number (KHN) was then calculated and analysed.

4.1 Study Materials

4.1.1 Resin-Based Composites

Two bulk-fill RBCs (Figure 4.1) of different matrix composition and photoinitiators were used in this study. The first material was Tetric N Ceram® Bulk Fill (TN) (Ivoclar Vivadent, Schaan, Liechtenstein) which has CQ and Ivocerin® photoinitiators, providing it with a wide absorption range between 370 nm and 460 nm. Filtek™ Bulk Fill (FK) (3M ESPE, St. Paul, MN, USA) was the second material assessed which uses only CQ photoinitiator giving it a narrower absorption range between 410 nm and 500 nm. Table 4.1 shows the technical profile and composition of the two restorative materials.

4.1.2 Light Curing Unit

A polywave LED LCU (Bluephase® N, Ivoclar Vivadent, Schaan, Liechtenstein); (Figure 4.2) was used. It features blue and violet colour components and a 10 mm black light probe. It has three different curing modes; high power, low power and soft start. In this study, the high-power mode (1200 mW/cm^2) was used. The technical profile of the LCU is shown in Table 4.2.

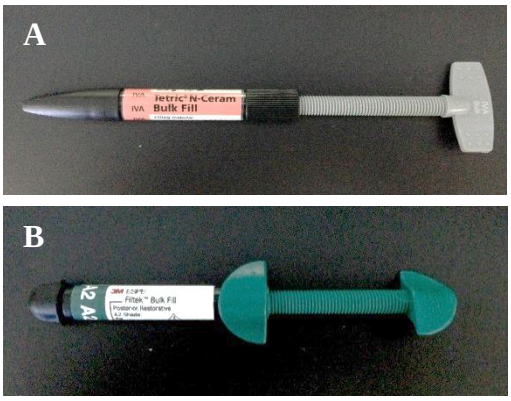

Figure 4.1: Bulk-fill resin-based composites – A, Tetric N Ceram® Bulk Fill; **B**, Filtek™ Bulk Fill

Figure 4.2: Light curing unit – Bluephase® N

Table 4.1: Technical profiles of the bulk-fill RBCs

Material	Manufacturer	Matrix	Filler Type	Filler Load		Photoinitiator
				wt. %	vol.%	
Tetric N Ceram®	Ivoclar Vivadent, Inc., NY, USA	Bis-GMA Bis-EMA UDMA (21 wt% organic matrix in total)	Prepolymer fillers 17wt% Barium Aluminum Silicate glass filler Ytterbium trifluoride Spherical mixed oxide filler	75-77	53-55	Acyl phosphine oxide Camphorquinone Dibenzoyl germanium derivative (Ivocerin®)
Filtek™ Bulk Fill	3M ESPE, St. Paul, MN, USA	AUDMA UDMA DDDMA	Silica fillers Zirconia fillers Zirconia/Sil-ica fillers Ytterbium Triflouride	76.5	58.4	Camphorquinone

Bis-GMA = Bisphenol-A glycidyl methacrylate
Bis-EMA = Ethoxylated bisphenol-A-glycidyl methacrylate
UDMA = Urethane Dimethacrylate
AUDMA = high molecular weight aromatic dimethacrylate
DDDMA = 1, 12-Dodecanediol dimethacrylate

Table 4.2: Technical Profile of the LCU

Light Curing Unit	Manufacturer	Type	Intensity (mW/cm^2)	Range Wavelength(s) (nm)
Bluephase® N	Ivoclar Vivadent, Schaan, Liechtenstein	Polywave	~1200 ±10%	(385 - 515) nm

4.1.3 Acrylic Perspex® Moulds

Black customized acrylic Perspex® sheets were used to prepare the moulds for RBC sample preparation. Acrylic Perspex® sheets were produced with outer dimensions of 45 mm x 15 mm x 4 mm (Figure 4.3.A). Three holes were drilled in each acrylic Perspex® sheet ((Figure 4.3.B). Subsequently, each sheet was sectioned into three equal parts to obtain a final acrylic Perspex® mould with outer dimensions of 15 mm x 15 mm x 4 mm and a single hole of 5 mm diameter in the centre (Figure 4.3.C).

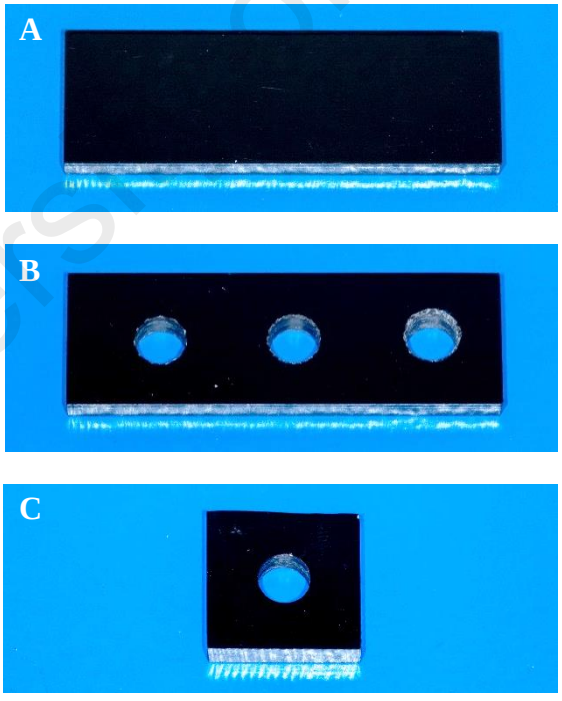

Figure 4.3: Steps of acrylic Perspex® mould preparation – **A**, Acrylic sheet (45 mm x 15 mm x 4 mm); **B**, Acrylic sheet with three 5 mm holes drilled; **C**, Final acrylic mould

4.1.4 Distance Blocks

To mount the LCU at different curing light distances from the surface of RBC, distance blocks were fabricated. This was performed by wrapping multiple glass slides of 0.80 mm thickness with an adhesive tape of 0.02 mm thickness to get the final desired distance. The final thickness of the distance blocks was confirmed using a digital calliper (Mitutoyo Corporation, Kawasaki, Japan) (Figure 4.4). A pair of distance blocks were assembled; the final thicknesses produced were 2 mm, 4 mm, 6 mm and 8 mm (Figure 4.5). A customized metal plate with a 10 mm diameter hole was fabricated (Figure 4.6). This rested on the distance blocks placed on each side to support the LCU guide at the desired curing light distance.

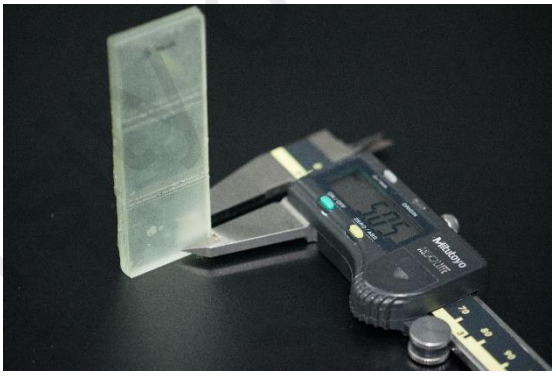

Figure 4.4: Measuring a distance block with a digital calliper

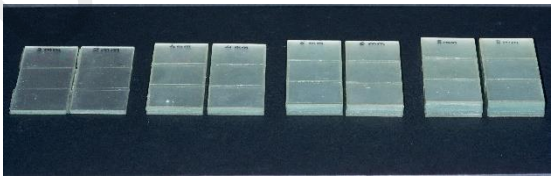

Figure 4.5: Distance blocks with different thicknesses (2 mm, 4 mm, 6 mm and 8 mm)

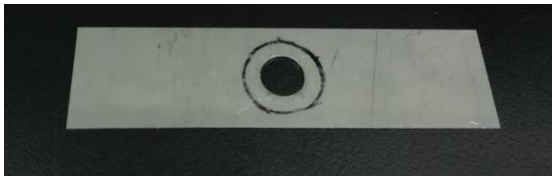

Figure 4.6: Metal plate with 10 mm diameter hole

During curing of the RBC samples, the moulds were placed on a 1 mm thick glass slide to obtain a flat bottom surface. A 1 mm glass slide was added to the 4 mm thick Perspex® mould to obtain a total distance of 5 mm from the base of the glass slide to the top surface of the RBC sample (Figure 4.7). The distance blocks prepared were used to set the distance from the top surface of the RBC sample to the LCU guide. Therefore, to compensate for the 5 mm of the glass slide and the mould height altogether, 5 mm distance blocks were prepared to be placed underneath different distance blocks during the experiment. Therefore, for example, if an 8 mm distance was needed between the top surface of RBC sample and the LCU guide, an 8 mm distance block was placed above a 5 mm distance block (Figure 4.8).

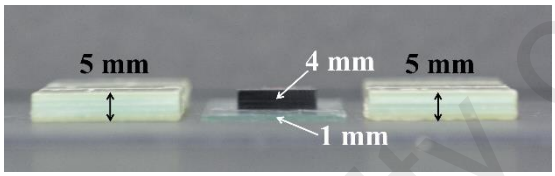

Figure 4.7: Side view of the assembled Perspex® mould on top of the 1 mm glass slide

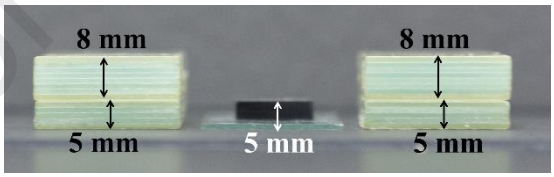

Figure 4.8: Placement of 8 mm distance block on top of 5 mm distance blocks

4.2 Sample Size Estimation

The sample size was calculated using G*Power software, version 3.0.10. A sample size of at least 6 in order to have 95% power of detecting the difference at 5% level of significance was needed. This was calculated based on data from a previous study (Rode et al., 2007) (α=0.05; power= 0.95). The final sample size was 12. Figure 4.9 shows a flow chart of the sample distribution.

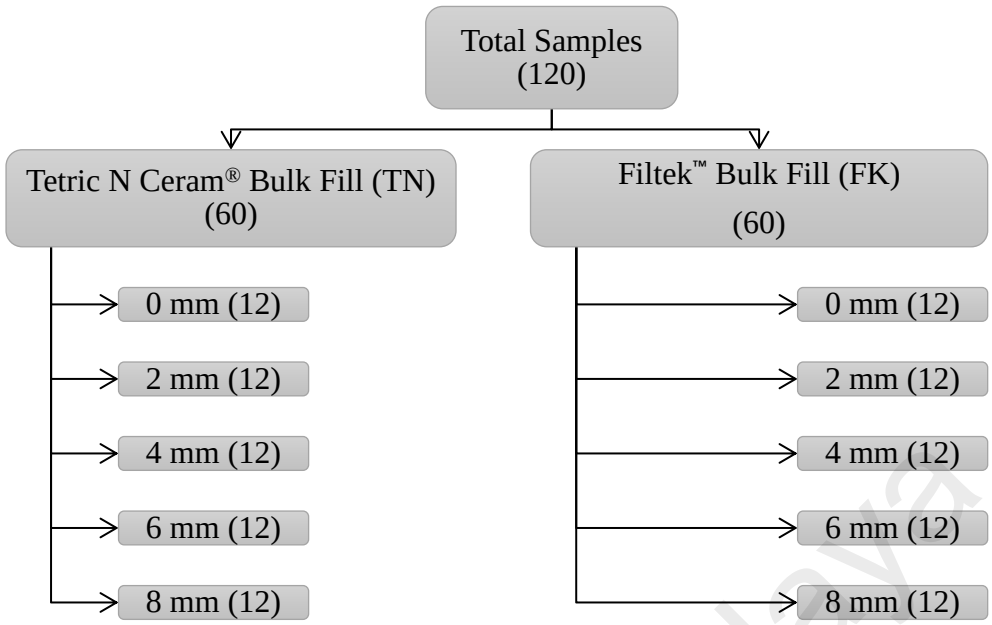

Figure 4.9: Sample distribution for each RBC at different distances

4.3 Specimen Preparation

4.3.1 Sample Preparation

RBC samples were prepared under ambient laboratory conditions at 23 ± 2 °C and 50 ± 10% relative humidity. The two base distance blocks (5 mm thickness) were placed on each side of a single glass slide (Figure 4.10). A transparent matrix strip (Ruwa Matrix Strips; Austenal Dental Products Ltd., Harrow, UK) was placed over the glass slide (Figure 4.11) followed by placement of acrylic mould over it (Figure 4.12). The bulk-filled RBC was packed inside the mould in a single increment using a hand instrument (Dentsply, Caulk, Milford, DE, USA) (Figure 4.13). Another matrix strip was placed on the top of the mould to exclude oxygen contamination (Figure 4.14). The RBC material was pressed with a glass slide using finger pressure to extrude excess material (Figure 4.15). The top glass slide was removed; however, the matrix strip was kept in place during the photopolymerization of the samples.

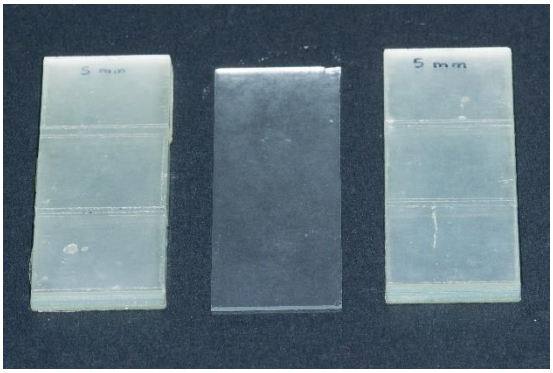

Figure 4.10: Base distance blocks and a single glass slide in the middle

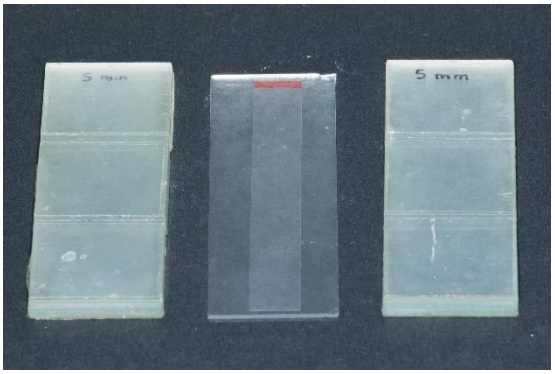

Figure 4.11 A matrix strip placed over the glass slide

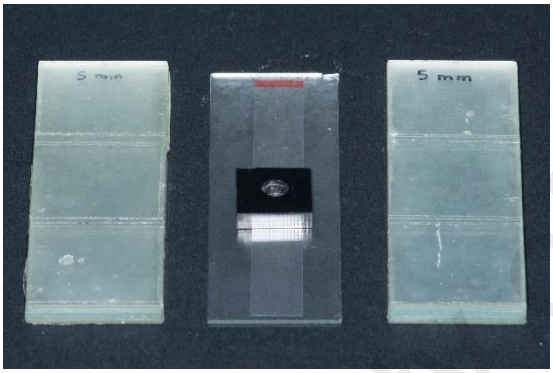

Figure 4.12: Acrylic mould placed over the matrix strip

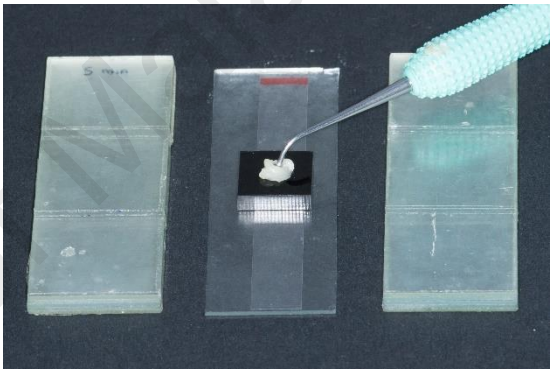

Figure 4.13: Packing of RBC in a single increment inside the mould

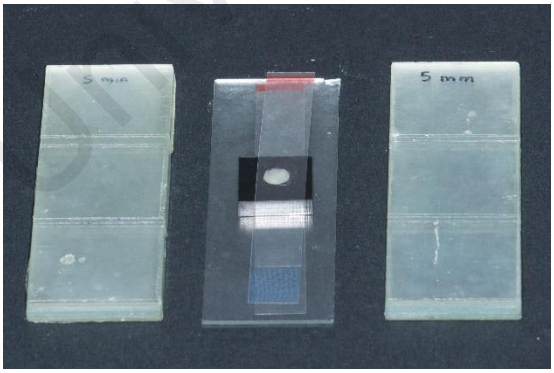

Figure 4.14: Placement of matrix strip on the top of the mould

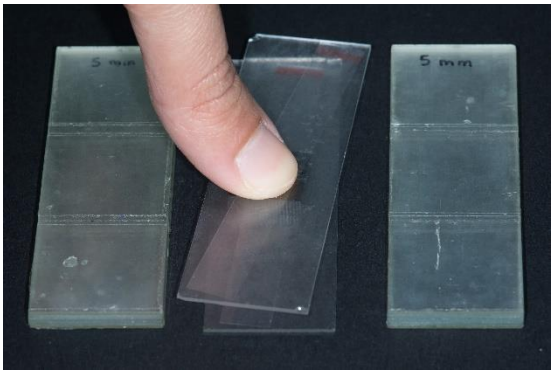

Figure 4.15: Application of finger pressure on the top surface of the sample

4.3.2 Curing Light Distance Adjustment

RBC photopolymerization was carried out at different distances (0 mm, 2 mm, 4 mm, 6 mm and 8 mm) according to the specified group. For 0 mm distance, the LCU exit window was placed against the top matrix strip directly. For the other distances, the distance blocks of the required curing light distance were added to the base distance blocks. The metal plate was supported by the distance blocks (Figure 4.16). The LCU guide was supported by the metal plate where the exit window was placed flush with the metal plate (Figure 4.17).

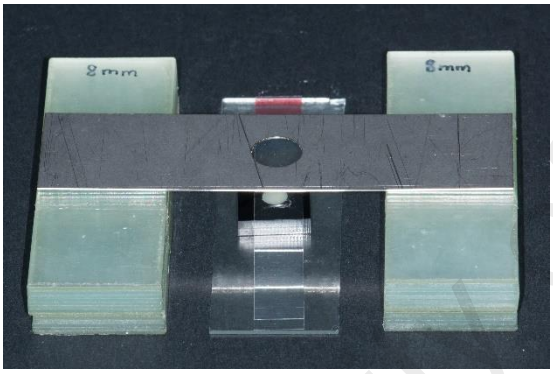

Figure 4.16: Placement of 8 mm distance block and resting the metal plate placed over it

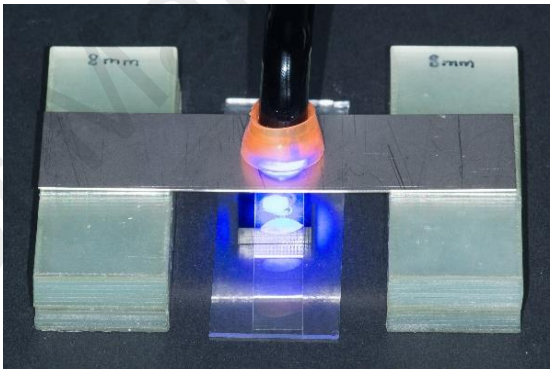

Figure 4.17: LCU guide supported on the metal plate

4.3.3 Curing Protocol

Samples were cured using a polywave LED LCU at high power mode emitting an irradiance of 1200 mW/cm^2. The LCU was fully charged before every use and the irradiance was verified to be at least 1000 mW/cm^2 at the beginning and the end of each day of specimen preparation with a dental radiometer ((Bluephase Meter II, Ivoclar Vivadent, Schaan, Liechtenstein) (Figure 4.18). The samples were photopolymerized for 20 seconds from the top surface of the material. The exit window of the LCU was centred over the samples during photopolymerization and the same direction of the curing light guide was maintained for all samples.

4.3.4 Specimen Storage

After polymerization, the specimen dimensions were measured using the digital calliper, ensuring that the specimen height was 4.0 mm ± 0.20 mm. Subsequently, specimens were immediately stored in complete darkness using a lightproof box to avoid further exposure to light in 100% relative humidity in an incubator (Memmert Incubator IN450, Memmert GmbH 1 Co. KG, Schwabach, Germany) at 37 °C for 24 hours (Figure 4.19).

Figure 4.18: Dental radiometer used to measure LCU irradiance

Figure 4.19: Incubator used for storage of samples

4.4 Knoop Surface Hardness

Knoop SH indentation was made with a micro-indentation hardness testing machine (Shimadzu Corporation, Kyoto, Japan) (Figure 4.20). The machine was calibrated at the start of each day before use. RBC samples were kept in the acrylic Perspex® mould to ensure a perpendicular surface to the micro-indenter during measurements. Three micro-indentations were made on the top surface and the bottom surface of each specimen using 10 gm load for 10 seconds and 40x magnification (Figure 4.21). The first micro-indentation was placed at the centre of each surface. Two micro-indentations were then made on either side of the first micro-indentation. A distance of 200 µm was maintained between each micro-indentation.

Micro-indentation length was measured digitally from stored images (Shimadzu HMV software, version 1.10, Shimadzu Corporation, Japan) (Figure 4.22) and Knoop hardness number (KHN) values were then calculated on the software from the measurements obtained. Figure 4.23 shows a schematic diagram for Knoop indentation. KHN was automatically calculated by the software using the formula:

$$KHN = 14.229\frac{F}{D^2}$$

Where

KHN = Knoop hardness number;

F = force in Newtons (0.98N) and

D = length of longer diagonal in µm.

Figure 4.20: Surface hardness micro-indentation testing machine

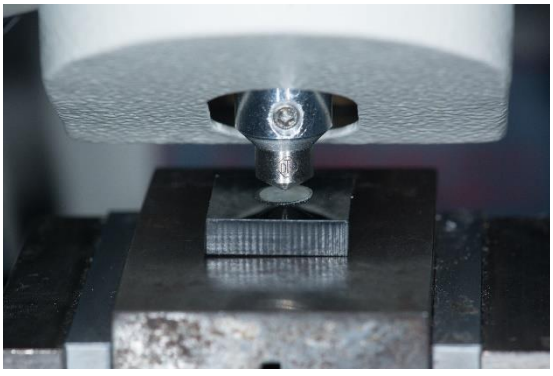

Figure 4.21: Knoop micro-indentation on the top surface of RBC

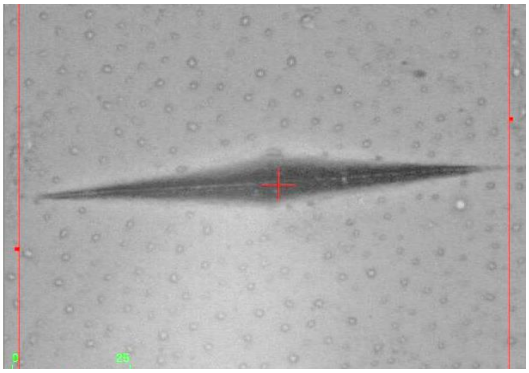

Figure 4.22: Knoop micro-indentation

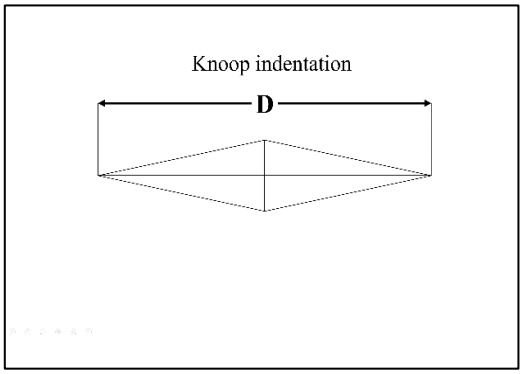

Figure 4.23: A schematic diagram showing the longer diagonal of Knoop micro-indentation

4.5 Data Analysis

SPSS version 23.0 (IBM SPSS Inc, Chicago, IL, USA) was used to analyse SH and HR data. Normality testing was performed using the Shapiro-Wilk test. Data were found to be normally distributed. Levene's test was performed and the results indicated that the variances among groups were homogenous. Consequently, one-way analysis of variance (ANOVA) and Tukey's post hoc test were used to determine the effect of curing light distance on the top SH, the bottom SH and the HR of each bulk-fill RBC. Following that, inter-material comparisons were carried out using independent sample t-test. Significance level was set at α=0.05.

CHAPTER 5: RESULTS

5.1 Descriptive Statistics

In this study, there were a total of five groups for each RBC material. For each sample, the SH value was measured three times for each of the top and bottom surfaces. The mean value for each surface was calculated (Table 5.1).

Table 5.1: Mean top SH, bottom SH and HR values

Curing Light Distance	Tetric N Ceram® Bulk Fill (TN)			Filtek™ Bulk Fill (FK)		
	Top SH (SD)	Bottom SH (SD)	HR (SD)	Top SH (SD)	Bottom SH (SD)	HR (SD)
D0	35.44 (3.60)	16.39 (1.77)	0.46 (0.05)	44.76 (1.68)	35.41 (4.69)	0.79 (0.11)
D2	41.24 (3.05)	17.56 (3.65)	0.43 (0.09)	50.07 (2.61)	37.48 (3.73)	0.75 (0.07)
D4	38.13 (5.33)	16.89 (1.35)	0.45 (0.08)	51.12 (2.85)	37.60 (3.09)	0.74 (0.08)
D6	38.50 (2.11)	14.15 (1.51)	0.37 (0.05)	46.67 (3.18)	34.14 (3.01)	0.73 (0.08)
D8	34.54 (2.89)	9.12 (1.14)	0.27 (0.04)	48.17 (4.48)	32.57 (3.19)	0.68 (0.07)

The mean SH for TN ranged between 34.45 and 41.24 for the top surface and between 9.12 and 17.56 for the bottom surface. The HR ranged from 0.27 to 0.46. However, for FK, the mean SH was between 44.76 to 51.12 and from 32.57 to 37.60 for the top and bottom surfaces respectively. The HR of FK ranged from 0.68 to 0.79. The highest mean SH values for top and bottom surface was noted at curing light distance 2 mm and 4 mm for TN and FK respectively. The highest mean HR was noted at curing light distance 0 mm for both RBCs.

5.2 Comparison of Mean Top SH for Each RBC

One-way ANOVA showed that there was a significant difference in the top SH mean values between the different groups of TN and FK (Table 5.2). For TN, the top SH mean values at curing light distance 2 mm (M = 41.24, SD = 3.05) was statistically higher in comparison to 0 mm (M = 35.44 , SD = 3.60) and 8 mm (M = 35.54, SD = 2.89). However, for FK, the top SH mean values at curing light distance 0 mm (M = 44.76, SD = 1.68) was statistically lower in comparison to 2 mm (M = 50.07 , SD = 2.60), 4 mm (M = 51.12, SD = 2.85), and 8 mm (M = 48.17, SD = 3.48). In addition, at 6 mm (M = 46.67, SD = 3.18) curing light distance, the top SH mean values was lower than that of 2 mm and 4 mm curing light distance.

Table 5.2: Comparison of mean values of top SH between groups of TN and FK

Curing Light Distance	D0	D2	D4	D6	D8	*F*	*p**	η^2
	Mean (SD)	Mean (SD)	Mean (SD)	Mean (SD)	Mean (SD)			
TN	35.44^{a} (3.60)	41.24^{b} (3.05)	38.13^{ab} (5.33)	38.50^{ab} (2.11)	34.54^{a} (2.89)	6.702	< 0.001	0.328
FK	44.76^{a} (1.68)	50.07^{b} (2.61)	51.12^{b} (2.85)	46.67^{ac} (3.18)	48.17^{bc} (4.48)	9.825	< 0.001	0.417

*One-way ANOVA, *significant at p<0.05*
*Tukey's post hoc test, *significant at p<0.05*
Mean values with differing subscripts within rows are significantly different

5.3 Comparison of Mean Bottom SH for Each RBC

One-way ANOVA showed statistically significant difference of the bottom SH mean values between the different groups of TN and FK (Table 5.3). Tukey's HSD test results showed that the mean values of bottom SH values of TN at curing light distance at 6 mm (M = 14.15, SD = 1.51) was statistically lower than the bottom SH mean values at curing light distances 2 mm (M = 17.56, SD = 3.65) and 4 mm (M = 16.89, SD = 1.35).

Additionally, the bottom SH mean values at 8 mm (M = 9.12, SD = 1.14) was statistically significantly lower than all the other curing light distances; 0 mm (M = 16.39, SD = 1.77), 2 mm (M = 17.56, SD = 3.65), 4 mm (M = 16.89, SD = 1.35) and 6 (M = 14.15, SD = 1.51). For FK, the bottom SH mean values at curing light distance 8 mm (M = 32.57, SD = 3.19) was statistically lower in comparison to 2 mm (M = 37.48 , SD = 3.73) and 4 mm (M = 37.60, SD = 3.09).

Table 5.3: Comparison of mean values of bottom SH between groups of TN and FK

Curing Light Distance	D0	D2	D4	D6	D8	*F*	*p**	η^2
	Mean (SD)	Mean (SD)	Mean (SD)	Mean (SD)	Mean (SD)			
TN	16.39^{ab} (1.77)	17.56^{a} (3.65)	16.89^{a} (1.35)	14.15^{b} (1.51)	9.12^{c} (1.14)	32.399	< 0.001	0.702
FK	35.41^{ab} (4.69)	37.48^{a} (3.73)	37.60^{a} (3.09)	34.14^{ab} (3.01)	32.57^{b} (3.19)	4.345	0.004	0.240

*One-way ANOVA, *significant at p<0.05*
*Tukey's post hoc test, *significant at p<0.05*
Mean values with differing subscripts within rows are significantly different

5.4 Comparison of Mean HR for Each RBC

A significant difference in SH was noted between different curing light distances (Table 5.4). For TN, curing light distance 6 mm (M = 0.37, SD = 0.05), the HR was statistically lower in comparison to 0 mm (M = 0.46, SD = 0.05) and 4 mm (M = 0.45, SD = 0.08). In addition, curing light distance at 8 mm (M = 0.27, SD = 0.04) was statistically lower than all other distances; 0 mm (M = 0.46, SD = 0.05), 2 mm (M = 0.43, SD = 0.09), 4 mm (M = 0.45, SD = 0.08) and 6 mm (M = 0.37, SD = 0.05). However, for FK, the only statistical significance between groups was noted between curing light distance 0 m (M = 0.79, SD = 0.11) which was higher than HR of curing light distance 8 mm (M = 0.68, SD = 0.07).

Table 5.4: Comparison of mean values of HR between groups of TN and FK

Curing Light Distance	D0	D2	D4	D6	D8	*F*	*p**	η^2
	Mean (SD)	Mean (SD)	Mean (SD)	Mean (SD)	Mean (SD)			
TN	0.46^{a} (0.05)	0.43^{ab} (0.09)	0.45^{a} (0.08)	0.37^{b} (0.05)	0.27^{c} (0.04)	19.471	< 0.001	0.586
FK	0.79^{a} (0.11)	0.75^{ab} (0.07)	0.74^{ab} (0.08)	0.73^{ab} (0.08)	0.68^{b} (0.07)	2.957	0.028	0.177

*One-way ANOVA, *significant at p<0.05*
*Tukey's post hoc test, *significant at p<0.05*
Mean values with differing subscripts within rows are significantly different

5.5 Comparison of SH and HR Between TN and FK

The independent sample t-test showed a statistically significant difference in the mean values of top SH, bottom SH and HR between TN and FK at different groups (Figures 5.1 to 5.3)

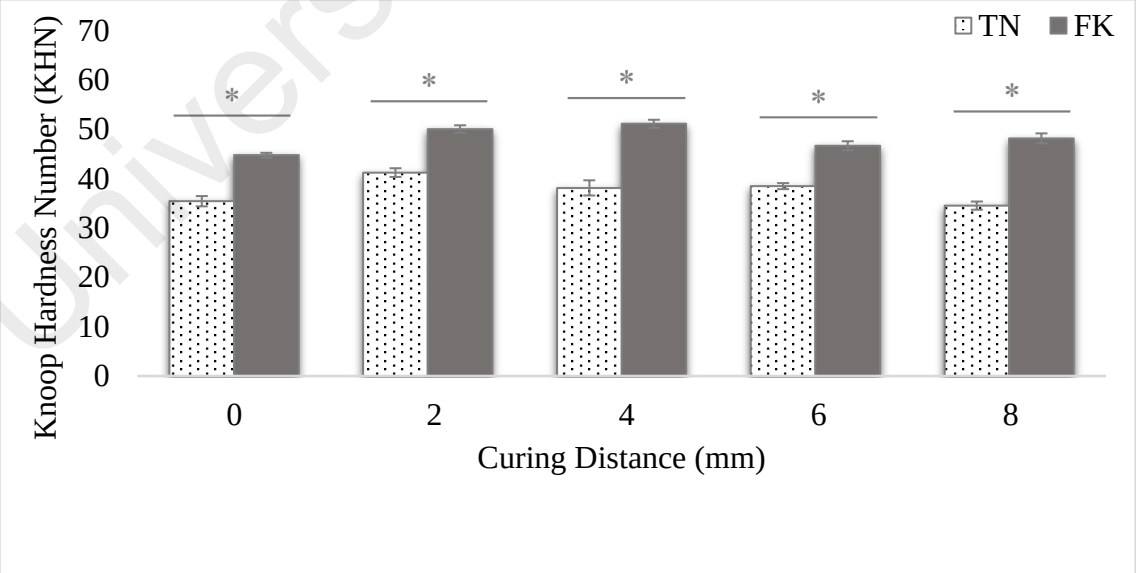

Figure 5.1: Top SH values for TN and FK (* *p*< 0.05)

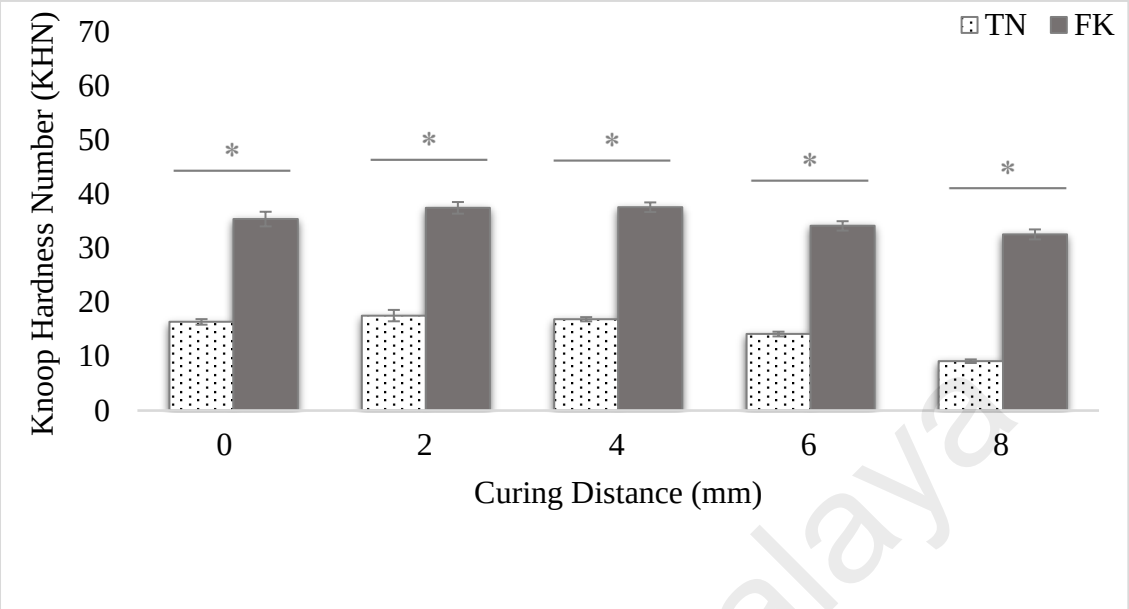

Figure 5.2: Bottom SH values for TN and FK (* $p < 0.05$)

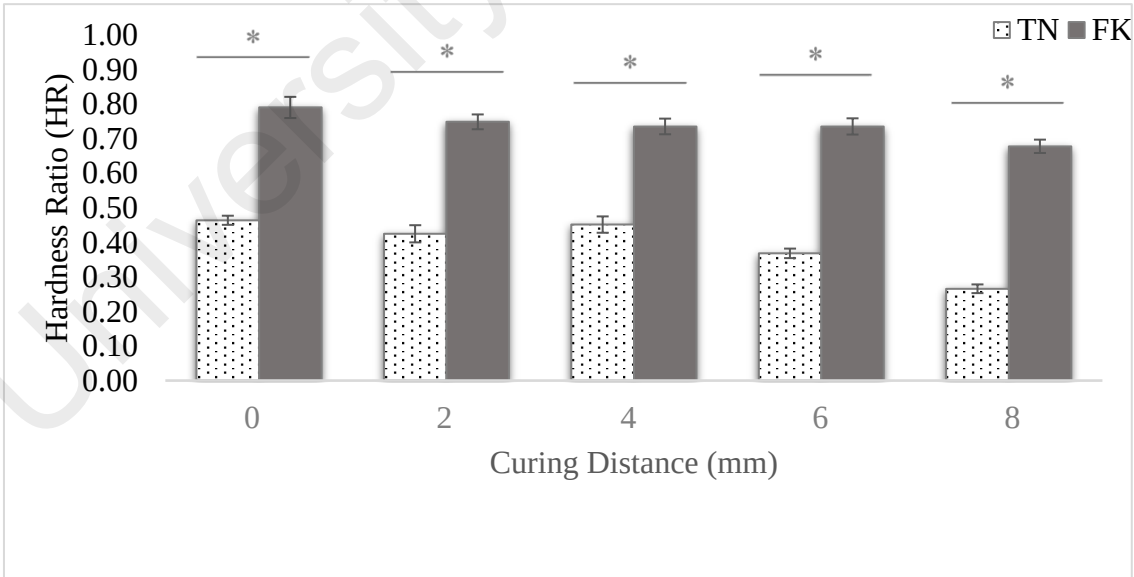

Figure 5.3: HR values for TN and FK (* $p < 0.05$)

5.6 Summary of the Statistical Analysis

Tables 5.5 shows an overview of the SH and HR results for TN and FK.

Table 5.5: Statistical analysis of SH at different curing light distances

Materials	**TN**		**FK**	
	Ranking	**Results***	**Ranking**	**Results***
Top SH	D2 > D4 > D6 > D0 > D8	D2 > D0, D8	D4 > D2 > D8 > D6 > D0	D2, D4, D6 > D0 D2, D4 > D6
Bottom SH	D2 > D4 > D0 > D6 > D8	D2, D4 > D6 D0, D2, D4, D6 > D8	D4 > D2 > D0 > D6 > D8	D2, D4 > D8
HR	D0 > D4 > D2 > D6 > D8	D0, D4 > D6 D0, D2, D4, D6 > D8	D0 > D2 > D4 > D6 >D8	D0 > D8

*One-way ANOVA, *significant at p<0.05*
*Tukey's post hoc test, *significant at p<0.05*
Abbreviations: SH, Surface hardness; TN, Tetric N-Ceram Bulk Fill; FK, Filtek™ Bulk Fill.

CHAPTER 6: DISCUSSION

6.1 Introduction

The results of the current study show that the distance between the LCU guide and the RBC restoration influence the top and the bottom SH of bulk-fill RBC. Additionally, the effectiveness of cure of bulk-fill RBCs was affected by different curing light distances. The tested materials did not meet the recommended HR value of 0.80. The effectiveness of cure of bulk-fill RBC is found to be material dependent. Therefore, all the null hypotheses are rejected.

Effectiveness of cure of RBCs was used to describe the extent of polymerization reaction of the material (Yap & Seneviratne, 2001). It dictates many physical and mechanical properties of the RBC (Asmussen, 1982a). To ensure optimum restoration properties and prolonged clinical performance, RBC should be photopolymerized under ideal conditions. Maximum LCU radiant exposure should be delivered to the restoration for ultimate polymerization to yield to enhanced effectiveness of cure (Price, Felix, & Andreou, 2004).

Clinically, ideal conditions are difficult to obtain due to the interaction of multiple factors related to RBC as well as LCU. The curing light guide should be placed perpendicular and as close as possible to the restoration to deliver a homogenous light beam with minimum light attenuation (Konerding et al., 2016). However, maintaining close proximity of the curing light guide to the surface of RBC is difficult and sometimes impossible. The cusp height of posterior teeth, the shape and/or size of the curing light guide and the use of separation rings or matrices contribute to this difficulty. Furthermore, the presence of Class II proximal cavity where the average depth ranges between 4 mm to 7 mm and in some occasions, it even reach more than 8 mm (Hansen & Asmussen, 1997; Price et al., 2000). To stimulate different clinically relevant situations, curing light

distances of 0 mm, 2 mm, 4 mm, 6 mm and 8 mm were used in the current study. The curing light distance of 8 mm was selected for extensive investigation of clinically challenging situations where the possibility of deep proximal cavity depth of more than 8 mm is presented with an added difficulty of reaching the posterior tooth.

6.2 Experimental Design of the Study

The current laboratory study investigated two bulk-fill RBCs photopolymerized with a polywave LCU under five different curing light distances. Great care was taken to mimic the clinical situation as much as possible. Different mould of varying materials, colours and translucency such as stainless-steel rings (Alrahlah et al., 2014; Shibasaki et al., 2017), acrylic Delrin® moulds (Yap, Wong, & Siow, 2003), Teflon or Polytetrafluoroethylene (PTFE) moulds (Flury, Peutzfeldt, & Lussi, 2014; Yokesh, Hemalatha, Muthalagu, & Justin, 2017), or extracted human teeth (Campodonico, Tantbirojn, Olin, & Versluis, 2011; Singhal, Gurtu, Singhal, Bansal, & Mohan, 2017) have been used to prepare RBC samples. The material and the colour of the mould has a significant impact on the final results (AlShaafi, AlQussier, AlQahtani, & Price, 2018; Harrington & Wilson, 1993; Price, Rueggeberg, Harlow, & Sullivan, 2016). LCU radiation is transmitted through both the restorative and the mould material. Exaggerated depths of cure are obtained when white PTFE moulds were used. Hence, in order to obtain meaningful comparative values for various products and shades, the use of a black or stainless-steel mould was recommended (Harrington & Wilson, 1993). Stainless-steel moulds absorb more light in comparison to Teflon or Delrin® moulds (Erickson & Barkmeier, 2017). And for extracted human natural teeth, standardization between samples was unfeasible. There were also no experimental studies comparing extracted human natural teeth to other mould types (Alshihri et al., 2018). Therefore, black acrylic

moulds were chosen for the current study. The final outer dimensions of the mould allowed mounting on the Knoop hardness indenter ensuring a perpendicular surface of the sample surface to the indenter. The final mould contained a single hole in the centre for single sample preparation. This ensured the elimination of undesirable light exposure in case three holes were mounted on the same acrylic sheet.

Matrix strips were used during sample preparation to minimize the formation of the oxygen-inhibition layer and to produce a flat and smooth surface. This allows the ease of indentation measurement and eliminates the need for polishing. Surface polishing of the sample has been done in several earlier studies (Bucuta & Ilie, 2014; Ilie, Kessler & Durner, 2013b). However, in the current study polishing was avoided to eradicate the effect of heat friction produced during polishing which might alter the properties of the material (Chinelatti, Chimello, Ramos, & Palma-Dibb, 2006; Vankerckhoven, Lambrechts, van Beylen, Davidson, & Vanherle, 1982). Samples were cured for 20 seconds through the matrix strip from the top surface. Although TN manufacturer recommended photopolymerization for 10 seconds, a pilot study revealed that the surface of the samples was too soft to allow KHN micro-indentation to be made.

The LCU was fully charged before each use to ensure maximum radiant exposure is delivered to the samples. Low battery levels of LED LCUs decrease the LCU intensity (Tongtaksin & Leevailoj, 2017) which can influence some properties of RBCs (Pereira et al., 2016). It was reported that after 25 exposures in a row, the radiant exposure might decrease between 2% and 8% (Andre, Nima, Sebold, Giannini, & Price, 2018). Following the manufacturer's instructions, the light irradiance was verified to be at least 1000 mW/cm^2. Therefore, at the beginning and the end of each day of specimen preparation, the irradiance was measured using a portable dental spectrometer (CureRite, Dentsply, Caulk). It was found that the values recorded with a portable spectrometer instrument

closely matched the 'gold standard' of the integrating sphere apparatus calibrated according to International Standards (Shortall, Felix, & Watts, 2015).

Bluepahse N® LCU has three blue lights and one violet light in its curing light guide. These lights are not arranged symmetrically hence producing asymmetrical beam profile. Therefore, to ensure standardization during sample photopolymerization and SH measurements, the direction of the mould in relation to the LCU guide was recorded and maintained for all samples. This was done by marking the side of the mould that was in alignment with the body of the LCU. This ensured the placement of the moulds on the Knoop hardness micro-indenter testing machine was consistent; therefore, the sites of the micro-indentions were almost identical among different samples.

The effectiveness of cure can be assessed directly by obtaining the DC of the material or indirectly by measuring the SH. DC has been directly correlated with the mechanical properties of the RBCs (Asmussen, 1982a; Ferracane, 1985). SH is widely used which might be due to the relatively uncomplicated sample preparation technique and the use of less expensive equipment compared to the complex and costly FTIR method. Knoop SH was proved to be the best predictor for DC ($r = 0.97$) where it was found that as SH increases, its DC increases (Rueggeberg & Craig, 1988). Thus, if a sample DC increased at a rapid rate, there would be a very steep rise in hardness values, making this parameter a very sensitive predictor of conversion (Rueggeberg & Craig, 1988). Additionally, a significant correlation was found between the volume fraction of filler and Knoop hardness. No correlation, however, was found between the DC and the mechanical properties of the resinous matrix (Chung & Greener, 1990). In the current study, Knoop SH micro-indentations were made using a 10 gm load for ten seconds. These settings were selected after performing a pilot study on multiple samples. When higher force or prolonged time was applied, it was noticed that the micro-indentation was too big and its

borders were out of focus to have a reading. It should be noted that the principle of KHN reading is based on a micro-indentation in three- dimensions, and therefore the load and duration of Knoop SH micro-indentation do not affect the final readings as the same value will be obtained.

6.3 The Influence of Curing Light Distance on the Effectiveness of Cure

Increasing the distance between the LCU guide and the top surface of RBC samples results in a reduction in the light irradiance (Corciolani, Vichi, Davidson, & Ferrari, 2008; Price et al., 2000) due to amplified light attenuation which consequently decreases the power density of the light (Meyer et al., 2002; Pires et al., 1993). This results in a decrease of SH and DC of conventional RBCs (Aguiar et al., 2005; Pires et al., 1993; Rode et al., 2007; Vandewalle et al., 2005).

It is expected that the closer the distance between the curing light guide and surface of the samples, the higher the SH values. However, for both tested bulk-fill RBCs, there was no consistent relationship. For instance, at 2 mm curing light distance for TN, the highest top and bottom SH values were recorded. However, for FK, the highest SH values were recorded at 4 mm curing light distance. Even though the LCU direction in relation to the samples and SH micro-indenter was maintained during the experimental procedure, it should be noted that the light beam is inhomogeneous. Modern LED LCUs uses multiple LED chipsets which makes bundling the light more difficult resulting in an inhomogeneous beam profile and non-uniform irradiance distribution across their emitting curing light guide (Price, Labrie, Rueggeberg, & Felix, 2010). This means that not every point on an irradiated RBC surface gets exposed to the same level of irradiation from the different wavelengths, especially at different depths of the RBC (Michaud, Price,

Labrie, Rueggeberg, & Sullivan, 2014). This might have led to the inconsistent trend between the curing light distance and the SH.

The SH of the top and bottom surface of TN and FK showed lower mean values at 0 mm in comparison to 2 mm and 4 mm. FK top SH at 0 mm was even lower than 6 mm and 8 mm. Since the polymerization reaction is a diffusion-controlled reaction (Anseth et al., 1994), receiving the full energy of the LCU beam might have led to a rapid increase in the material viscosity limiting the diffusion rate of growing chains at 0 mm curing light distance. This would have led to less cross-linking and hence, lower SH values. In contrast, at curing light distances 2 mm or 4 mm, light has dispersed in the air yielding to a loss of energy dose which might have led to less photoinitiator excitation. This would have led to a decrease in chain cross-linking and therefore allowed more diffusion inside the polymer network, making the polymer more susceptible to the plasticization effect. This might be similar to a phenomenon observed in previous studies where the maximum SH was not reached at the first measuring depth of 0.1 mm. However, the subsurface areas at a depth of 0.2 mm to 1 mm were higher (Flury et al., 2012). These higher values were even observed at a depth of up to 2mm (Ilie et al., 2013b). The rate of diffusion of the growing chains is the most plausible explanation for this phenomenon.

The top SH was less dependent on curing light distance and was a poor indicator of bottom SH. This is in agreement with a similar study done on conventional RBCs (Pires et al., 1993). All the experimental groups of the current study showed considerably higher SH values at the top surface in comparison to the bottom surface. Similar findings were observed in conventional RBCs when the influence of curing light distance on the SH was investigated (Aguiar et al., 2005; Pires et al., 1993; Sobrinho et al., 2000). This was reported for bulk-fill RBCs as well (Farahat, Daneshkazemi, & Hajiahmadi, 2016; Malik & Baban, 2014; Moharam, El-Hoshy, & Abou-Elenein, 2017). This may be attributed to

the delivery of sufficient radiant exposure at the top surface in comparison to the bottom surface. Light beam scattering occurred inside the 4 mm-thick RBC samples which resulted in the lower light intensity at the bottom surface. The amount of light transmitted through an RBC is dependent on the amount of scattered and absorbed light (Musanje & Darvell, 2006). RBC shade and fillers size and distribution were found to affect the transmission of light through the material affecting the effectiveness of cure (Guiraldo et al., 2009; Jeong et al., 2009).

The DC of monomers into polymers within the RBC generally decreases from the surface of the restoration inwardly. As a result, the apparent hardness of the top or external surface is not an adequate indicator of complete material polymerization. Therefore, the bottom to top HR (B/T ratio) is calculated to assess the effectiveness of the cure of RBC. If the polymerization is completely effective, the HR should be one, as the hardness of the bottom surface should be identical to that of the top surface. An HR value of 0.80-0.90 is scientifically supported to be a reliable value for the effectiveness of cure (Johnston et al., 1985; Skeeters, Timmons, & Mitchell, 1983)

In the current study, increasing the curing light distance resulted in a negative influence on the effectiveness of cure of the tested bulk-fill RBCs. The HR at 0 mm curing light distance was the highest among the different groups. Similar findings were found in a study on conventional as well as bulk-fill RBCs (Aguiar et al., 2005; Farahat et al., 2016; Malik & Baban, 2014). None of the RBCs achieved the recommended value of 0.80. These findings are in agreement with a study done on bulk-fill RBCs where all the tested materials had an HR below 0.80 with the exception of SonicFill™ RBCs (Garcia et al., 2014). However, these findings are not in agreement with the results of other studies which found that all the tested bulk-fill RBCs reached an HR 0.80 (Alrahlah et al., 2014; Bucuta & Ilie, 2014). The results of other studies have equivocal findings where some

bulk-fill RBCs reached 0.80 while others did not reach the recommended value (Flury et al., 2012; Malik & Baban, 2014). This failure to meet the recommended values might be attributed to the high percentage of filler by weight in the current tested bulk-fill RBCs. This increased the light scattering and attenuation reducing the light intensity leading to decreased SH at the bottom surface of the samples (Ruyter & Oysaed, 1982).

As the curing light distance increased, the light irradiance decreased leading to a drop of HR. This is in agreement with a study that was done using power and energy analyser to assess the power output of different LED LCUs at different distances. It was reported that there was a tremendous drop in the power output with increasing the distance between the curing light guide and the analyser (Meyer et al., 2002). Light energy is absorbed as the light passes through the air. Additionally, it was found that the beam profile became inhomogeneous as the distance between the LCU guide and the analyzer increased (Roulet, Rocha, Shen, Khudhair, & Oliveira, 2018).

Overall, the SH of TN was significantly lower than that of FK. This is most likely due to the photoinitiator system used in each material, i.e, in TN was CQ and Ivocerin®, while in FK solely CQ. Therefore, FK has higher CQ content than TN which led to maximum light transmission and therefore improved the effectiveness of cure (Howard et al., 2010). Another possible explanation is the total inorganic filler content. The total inorganic filler volume excluding the pre-polymer fillers was lower in TN than in FK. Studies have shown a direct correlation between filler volume and mechanical properties, where the less the filler volume the lower the mechanical properties (Ilie & Hickel, 2009). The translucency of TN might have played a role in the lower values for TN compared to FK. The shade used for TN was IVA, which is a universal shade corresponding to shades A2 and A3. The shade used for FK was A2. Additionally, TN has Ivocerin® photoinitiator which contributes to a slightly higher RBC opacity compared to other bulk-fill materials

(Peschke, 2013). The incorporation of the additional photoinitiator Ivocerin® in TN was unable to compensate for the lower translucency in deeper layers resulting in a faster decrease in its polymerization kinetics (Ilie et al., 2013b).

Furthermore, as the refractive index difference between the resin and the filler narrows, the scattering coefficient decreases and transmission efficiency improves (Fujita et al., 2005). Upon photopolymerization, the refractive index of the resin increases linearly with conversion ($r^2 = 0.976$), producing a refractive index match between the resin and the filler at approximately 58 % conversion (Howard et al., 2010). This may explain the reason of the improved effectiveness of cure of FK in comparison to TN.

Photopolymerization of bulk-fill RBC is a complex process. No single explanation could be given for the obtained SH and HR values of the tested RBCs. A combination of factors leads to the general decrease in the effectiveness of cure with an increase in curing light distance. These factors would include the amount of fillers and photoinitiator type in the RBC. In addition, the properties of the light beam of the LCU in air and bulk-fill RBC also affected the overall results.

6.4 Limitations of the Study

Different direct and indirect techniques have been reported in the literature to measure the effectiveness of cure of RBCs. In the current study, SH which represents the indirect technique was used solely to assess the effectiveness of cure by evaluating the mechanical properties of the material. Direct methods such as FTIR measures DC by observing the decrease of the C=C double bonds during the polymerization reaction and can be used to determine the reaction kinetics. Although the SH and DC are correlated, it would have been better to perform both methods to assess the effectiveness of cure.

Another limitation of this study is the use of single polywave LED LCU. A variety of LCUs are available in the dental market with different irradiance output, different beam profiles and range of peak wavelengths emitted from their curing light guide. Different curing modes are also available. The current study used high irradiance output as the only curing mode for all the cured samples. The effect of the monowave LED LCU, as well as different curing modes, would have given additional information on the effect of the type of LCU on the SH.

Additionally, the tested materials were limited to two bulk-fill RBCs with single shade selected. A variety of bulk-fill RBCs are available in the market with different properties and would have generated additional information on the effectiveness of cure of bulk-fill RBCs with different properties. It should also be noted that properties measured under clinically simulated curing conditions might vary from those measured under ideal curing conditions.

CHAPTER 7: CONCLUSIONS

Under the test conditions of the current study, it can be concluded that:

- The top and bottom surface hardness of Tetric N Ceram® Bulk Fill and Filtek™ Bulk Fill are affected by the curing light distance. An inverse relationship is present between the curing light distance and the surface hardness of Tetric N Ceram® Bulk Fill when the curing light distance is equal to or more than 2 mm. This inverse relationship is present in Filtek™ Bulk Fill when the curing light distance is equal to or more than 4 mm.
- The hardness ratio for Tetric N Ceram® Bulk Fill and Filtek™ Bulk Fill resulted in a linear relationship independent of the filler size or loading. The effectiveness of cure decreased with the increase of the curing light distance.
- The effectiveness of cure of bulk-fill resin-based composites is material-dependent where Filtek™ Bulk Fill is cured more effectively than Tetric N Ceram® Bulk Fill. Therefore, the manufacturer's recommended total energy regimen may not always be adequate for effective curing.

CHAPTER 8: RECOMMENDATION

To complement the findings of the current research, the following future studies are suggested:

- Assessment of the SH using a wider range of bulk-fill RBCs at different curing light distances, compared to conventional systems.
- Assessment of the DC of different bulk-fill RBCs cured at different curing light distances and comparing them to conventional systems.
- Investigation of the relationship between the SH and the DC of bulk-fill RBCs at different curing light distances.
- Assessment of the SH and the DC of bulk-fill RBCs cured with different curing protocols as well as different curing durations.

REFERENCES

Aguiar, F. H., Lazzari, C. R., Lima, D. A., Ambrosano, G. M., & Lovadino, J. R. (2005). Effect of light curing tip distance and resin shade on microhardness of a hybrid resin composite. *Brazilian Oral Research, 19*(4), 302-306.

Al-Ahdal, K., Silikas, N., & Watts, D. C. (2014). Rheological properties of resin composites according to variations in composition and temperature. *Dental Materials, 30*(5), 517-524.

Alrahlah, A., Silikas, N., & Watts, D. C. (2014). Post-cure depth of cure of bulk fill dental resin-composites. *Dental Materials, 30*(2), 149-154.

AlShaafi, M. M., AlQussier, A., AlQahtani, M. Q., & Price, R. B. (2018). Effect of mold type and diameter on the depth of cure of three resin-based composites. *Operative Dentistry, 43*(5), 520-529.

Alshihri, A., Santini, A., & Aldossary, M. (2018). The Influence of in vitro Mold Characteristics on the Polymerization Outcomes of Resin Based Composites: A Literature Review. *Current Analaysis of Dentistry, 1*(2018), 7-11.

Andre, C. B., Nima, G., Sebold, M., Giannini, M., & Price, R. B. (2018). Stability of the light output, oral cavity tip accessibility in posterior region and emission spectrum of light-curing units. *Operative Dentistry, 43*(4), 398-407.

Andrzejewska, E., Lindén, L.-Å., & Rabek, J. F. (1998). The role of oxygen in camphorquinone-initiated photopolymerization. *Macromolecular Chemistry and Physics, 199*(3), 441-449.

Anseth, K. S., Wang, C. M., & Bowman, C. N. (1994). Kinetic evidence of reaction-diffusion during the polymerization ofmMulti(meth)acrylate monomers. *Macromolecules, 27*(3), 650-655.

Anusavice, K. J., Shen, C., & Rawls, H. R. (2012). *Philips Science of Dental Materials* (Twelfth ed.): Elsevier.

Asmussen, E. (1975). NMR-analysis of monomers in restorative resins. *Acta Odontologica Scandinavica, 33*(3), 129-134.

Asmussen, E. (1982a). Factors affecting the quantity of remaining double bonds in restorative resin polymers. *Scandinavian Journal of Dental Research, 90*(6), 490-496.

Asmussen, E. (1982b). Restorative resins: hardness and strength vs. quantity of remaining double bonds. *Scandinavian Journal of Dental Research, 90*(6), 484-489.

Benetti, A. R., Havndrup-Pedersen, C., Honore, D., Pedersen, M. K., & Pallesen, U. (2015). Bulk-fill resin composites: polymerization contraction, depth of cure, and gap formation. *Operative Dentistry, 40*(2), 190-200.

Beun, S., Glorieux, T., Devaux, J., Vreven, J., & Leloup, G. (2007). Characterization of nanofilled compared to universal and microfilled composites. *Dental Materials, 23*(1), 51-59.

Bichacho, N. (1994). The centripetal build-up for composite resin posterior restorations. *Practical Periodontics and Aesthetic Dentistry, 6*(3), 17-23; quiz 24.

Bouillaguet, S., Wataha, J. C., Hanks, C. T., Ciucchi, B., & Holz, J. (1996). In vitro cytotoxicity and dentin permeability of HEMA. *Journal of Endodontics, 22*(5), 244-248.

Bouschlicher, M. R., Rueggeberg, F. A., & Wilson, B. M. (2004). Correlation of bottom-to-top surface microhardness and conversion ratios for a variety of resin composite compositions. *Operative Dentistry, 29*(6), 698-704.

Bowen, R. L. (1956). Use of epoxy resins in restorative materials. *Journal of Dental Research, 35*(3), 360-369.

Bowen, R. L. (1959). Method of preparing a monomer having phenoxy and methacrylate groups linked by hydroxy glyceryl groups. United States patent US 3,179,623 A.

Bowen, R. L. (1962). Dental filling material comprising vinyl silane treated fused silica and a binder consisting of the reaction product of bis phenol and glycidyl acrylate. United States patent US 3,066,112 A.

Bowen, R. L. (1963). Properties of a silica-reinforced polymer for dental restorations. *Journal of the American Dental Association, 66*, 57-64.

Braga, R. R., Boaro, L. C., Kuroe, T., Azevedo, C. L., & Singer, J. M. (2006). Influence of cavity dimensions and their derivatives (volume and 'C' factor) on shrinkage stress development and microleakage of composite restorations. *Dental Materials, 22*(9), 818-823.

Bucuta, S., & Ilie, N. (2014). Light transmittance and micro-mechanical properties of bulk fill vs. conventional resin based composites. *Clinical Oral Investigations, 18*(8), 1991-2000.

Caldas, D. B., de Almeida, J. B., Correr-Sobrinho, L., Sinhoreti, M. A., & Consani, S. (2003). Influence of curing tip distance on resin composite Knoop hardness number, using three different light curing units. *Operative Dentistry, 28*(3), 315-320.

Campodonico, C. E., Tantbirojn, D., Olin, P. S., & Versluis, A. (2011). Cuspal deflection and depth of cure in resin-based composite restorations filled by using bulk, incremental and transtooth-illumination techniques. *Journal of the American Dental Association, 142*(10), 1176-1182.

Chinelatti, M. A., Chimello, D. T., Ramos, R. P., & Palma-Dibb, R. G. (2006). Evaluation of the surface hardness of composite resins before and after polishing at different times. *Journal of Applied Oral Science, 14*(3), 188-192.

Chung, K. H., & Greener, E. H. (1990). Correlation between degree of conversion, filler concentration and mechanical properties of posterior composite resins. *Journal of Oral Rehabilitation, 17*(5), 487-494.

Corciolani, G., Vichi, A., Davidson, C. L., & Ferrari, M. (2008). The influence of tip geometry and distance on light-curing efficacy. *Operative Dentistry, 33*(3), 325-331.

Cox, C. F., Keall, C. L., Keall, H. J., Ostro, E., & Bergenholtz, G. (1987). Biocompatibility of surface-sealed dental materials against exposed pulps. *Journal of Prosthetic Dentistry, 57*(1), 1-8.

Craig, R. G. (1981). Chemistry, composition, and properties of composite resins. *Dental Clinics of North America, 25*(2), 219-239.

Cramer, N. B., Stansbury, J. W., & Bowman, C. N. (2011). Recent advances and developments in composite dental restorative materials. *Journal of Dental Research*, *90*(4), 402-416.

Curtis, A. R., Palin, W. M., Fleming, G. J., Shortall, A. C., & Marquis, P. M. (2009). The mechanical properties of nanofilled resin-based composites: the impact of dry and wet cyclic pre-loading on bi-axial flexure strength. *Dental Materials, 25*(2), 188-197.

Czasch, P., & Ilie, N. (2013). In vitro comparison of mechanical properties and degree of cure of bulk fill composites. *Clinical Oral Investigations, 17*(1), 227-235.

Davidson, C. L. (1986). Resisting the curing contraction with adhesive composites. *Journal of Prosthetic Dentistry, 55*(4), 446-447.

de Moraes, R. R., Goncalves Lde, S., Lancellotti, A. C., Consani, S., Correr-Sobrinho, L., & Sinhoreti, M. A. (2009). Nanohybrid resin composites: nanofiller loaded materials or traditional microhybrid resins? *Operative Dentistry, 34*(5), 551-557.

de Oliveira, D., Rocha, M. G., Correa, I. C., Correr, A. B., Ferracane, J. L., & Sinhoreti, M. A. C. (2016). The effect of combining photoinitiator systems on the color and curing profile of resin-based composites. *Dental Materials, 32*(10), 1209-1217.

De Santis, A., & Baldi, M. (2004). Photo-polymerisation of composite resins measured by micro-Raman spectroscopy. *Polymer, 45*(11), 3797-3804.

Dentsply. (2011). SureFil SDR: posterior bulk fill flowable base.

Dionisio, J., Mahabadi, H. K., O'Driscoll, K. F., Abuin, E., & Lissi, E. A. (1979). High-conversion polymerization. IV. A definition of the onset of the gel effect. *Journal of Polymer Science: Polymer Chemistry Edition, 17*(7), 1891-1900.

Durner, J., Obermaier, J., Draenert, M., & Ilie, N. (2012). Correlation of the degree of conversion with the amount of elutable substances in nano-hybrid dental composites. *Dental Materials, 28*(11), 1146-1153.

Eick, J. D., & Welch, F. H. (1986). Polymerization shrinkage of posterior composite resins and its possible influence on postoperative sensitivity. *Quintessence International, 17*(2), 103-111.

El-Damanhoury, H., & Platt, J. (2014). Polymerization shrinkage stress kinetics and related properties of bulk-fill resin composites. *Operative Dentistry, 39*(4), 374-382.

Eliades, G. C., Vougiouklakis, G. J., & Caputo, A. A. (1987). Degree of double bond conversion in light-cured composites. *Dental Materials, 3*(1), 19-25.

Elliott, J. E., Lovell, L. G., & Bowman, C. N. (2001). Primary cyclization in the polymerization of bis-GMA and TEGDMA: a modeling approach to understanding the cure of dental resins. *Dental Materials, 17*(3), 221-229.

Erickson, R. L., & Barkmeier, W. W. (2017). Effect of mold diameter on the depth of cure of a resin-based composite material. *European Journal of Oral Sciences, 125*(1), 88-92.

Ernst, C. P., Meyer, G. R., Muller, J., Stender, E., Ahlers, M. O., & Willershausern, B. (2004). Depth of cure of LED vs QTH light-curing devices at a distance of 7 mm. *Journal of Adhesive Dentistry, 6*(2), 141-150.

Farahat, F., Daneshkazemi, A. R., & Hajiahmadi, Z. (2016). The effect of bulk depth and irradiation time on the surface hardness and degree of cure of bulk-fill composites. *Journal of Dental Biomaterials, 3*(3), 284-291.

Feilzer, A. J., De Gee, A. J., & Davidson, C. L. (1987). Setting stress in composite resin in relation to configuration of the restoration. *Journal of Dental Research, 66*(11), 1636-1639.

Ferracane, J. L., & Greener, E. H. (1984). Fourier transform infrared analysis of degree of polymerization in unfilled resins--methods comparison. *Journal of Dental Research, 63*(8), 1093-1095.

Ferracane, J. L. (1985). Correlation between hardness and degree of conversion during the setting reaction of unfilled dental restorative resins. *Dental Materials, 1*(1), 11-14.

Ferracane, J. L., & Condon, J. R. (1990). Rate of elution of leachable components from composite. *Dental Materials, 6*(4), 282-287.

Ferracane, J. L. (1994). Elution of leachable components from composites. *Journal of Oral Rehabilitation, 21*(4), 441-452.

Ferracane, J. L., & Mitchem, J. C. (2003). Relationship between composite contraction stress and leakage in Class V cavities. *American Journal of Dentistry, 16*(4), 239-243.

Ferracane, J. L. (2011). Resin composite--state of the art. *Dental Materials, 27*(1), 29-38.

Finger, W. J., Lee, K. S., & Podszun, W. (1996). Monomers with low oxygen inhibition as enamel/dentin adhesives. *Dental Materials, 12*(4), 256-261.

Flury, S., Hayoz, S., Peutzfeldt, A., Husler, J., & Lussi, A. (2012). Depth of cure of resin composites: is the ISO 4049 method suitable for bulk fill materials? *Dental Materials, 28*(5), 521-528.

Flury, S., Peutzfeldt, A., & Lussi, A. (2014). Influence of increment thickness on microhardness and dentin bond strength of bulk fill resin composites. *Dental Materials, 30*(10), 1104-1112.

Fouassier, J. P. (1995). *Photoinitiation, photopolymerization and photocuring: Fundamentals and Applications*: Hanser Publishers, Munich Vienna New York.

Fujita, K., Nishiyama, N., Nemoto, K., Okada, T., & Ikemi, T. (2005). Effect of base monomer's refractive index on curing depth and polymerization conversion of photo-cured resin composites. *Dental Materials Journal, 24*(3), 403-408.

Garcia, D., Yaman, P., Dennison, J., & Neiva, G. (2014). Polymerization shrinkage and depth of cure of bulk fill flowable composite resins. *Operative Dentistry, 39*(4), 441-448.

Gerzina, T. M., & Hume, W. R. (1996). Diffusion of monomers from bonding resin-resin composite combinations through dentine in vitro. *Journal of Dentistry, 24*(1-2), 125-128.

The Glossary of Prosthodontic Terms: Ninth Edition. (2017). *Journal of Prosthetic Dentistry, 117*(5S), e1-e105.

Goncalves, F., Azevedo, C. L., Ferracane, J. L., & Braga, R. R. (2011). BisGMA/TEGDMA ratio and filler content effects on shrinkage stress. *Dental Materials, 27*(6), 520-526.

Guiraldo, R. D., Consani, S., Consani, R. L., Berger, S. B., Mendes, W. B., & Sinhoreti, M. A. (2009). Light energy transmission through composite influenced by material shades. *Bulletin of Tokyo Dental College, 50*(4), 183-190.

Halvorson, R. H., Erickson, R. L., & Davidson, C. L. (2002). Energy dependent polymerization of resin-based composite. *Dental Materials, 18*(6), 463-469.

Hansen, E. K., & Asmussen, E. (1997). Visible-light curing units: correlation between depth of cure and distance between exit window and resin surface. *Acta Odontologica Scandinavica, 55*(3), 162-166.

Harrington, E., & Wilson, H. J. (1993). Depth of cure of radiation-activated materials--effect of mould material and cavity size. *Journal of Dentistry, 21*(5), 305-311.

Hassan, K., & Khier, S. (2005). Split increment horizontal layering: a simplified placement technique for direct posterior resin restorations. *General Dentistry, 53*(6), 406-409.

Heuer, G. A., Garman, T. A., Sherrer, J. D., & Williams, H. A. (1982). A clinical comparison of a quartz- and glass-filled composite with a glass-filled composite. *Journal of the American Dental Association, 105*(2), 246-247.

Howard, B., Wilson, N. D., Newman, S. M., Pfeifer, C. S., & Stansbury, J. W. (2010). Relationships between conversion, temperature and optical properties during composite photopolymerization. *Acta Biomaterialia, 6*(6), 2053-2059.

Ilie, N., & Hickel, R. (2009). Investigations on mechanical behaviour of dental composites. *Clinical Oral Investigations, 13*(4), 427-438.

Ilie, N., & Hickel, R. (2011). Investigations on a methacrylate-based flowable composite based on the SDR technology. *Dental Materials, 27*(4), 348-355.

Ilie, N., Rencz, A., & Hickel, R. (2013a). Investigations towards nano-hybrid resin-based composites. *Clinical Oral Investigations, 17*(1), 185-193.

Ilie, N., Kessler, A., & Durner, J. (2013b). Influence of various irradiation processes on the mechanical properties and polymerisation kinetics of bulk-fill resin based composites. *Journal of Dentistry, 41*(8), 695-702.

Ilie, N., Bucuta, S., & Draenert, M. (2013c). Bulk-fill resin-based composites: an in vitro assessment of their mechanical performance. *Operative Dentistry, 38*(6), 618-625.

International Organization for Standardization (2009). ISO4049: Dentistry Polymer-based filling, restorative and luting materials.

Jakubiak, J., Sionkowska, A., Lindén, L. Å., & Rabek, J. F. (2001). Isothermal Photo Differential Scanning Calorimetry. Crosslinking polymerization of multifunctional monomers in presence of visible light photoinitiators. *Journal of Thermal Analysis and Calorimetry, 65*(2), 435-443.

Jakubiak, J., Allonas, X., Fouassier, J. P., Sionkowska, A., Andrzejewska, E., Linden, L. Å., & Rabek, J. F. (2003). Camphorquinone–amines photoinitating systems for the initiation of free radical polymerization. *Polymer, 44*(18), 5219-5226.

Janda, R., Roulet, J. F., Kaminsky, M., Steffin, G., & Latta, M. (2004). Color stability of resin matrix restorative materials as a function of the method of light activation. *European Journal of Oral Sciences, 112*(3), 280-285.

Jang, J. H., Park, S. H., & Hwang, I. N. (2015). Polymerization shrinkage and depth of cure of bulk-fill resin composites and highly filled flowable resin. *Operative Dentistry, 40*(2), 172-180.

Jeong, T. S., Kang, H. S., Kim, S. K., Kim, S., Kim, H. I., & Kwon, Y. H. (2009). The effect of resin shades on microhardness, polymerization shrinkage, and color change of dental composite resins. *Dental Materials Journal, 28*(4), 438-445.

Johnston, W. M., Leung, R. L., & Fan, P. L. (1985). A mathematical model for post-irradiation hardening of photoactivated composite resins. *Dental Materials, 1*(5), 191-194.

Klapdohr, S., & Moszner, N. (2004). New Inorganic Components for Dental Filling Composites. *Monatshefte für Chemie - Chemical Monthly, 136*(1), 21-45.

Konerding, K. L., Heyder, M., Kranz, S., Guellmar, A., Voelpel, A., Watts, D. C., . . . Sigusch, B. W. (2016). Study of energy transfer by different light curing units into a class III restoration as a function of tilt angle and distance, using a MARC Patient Simulator (PS). *Dental Materials, 32*(5), 676-686.

Lagocka, R., Mazurek-Mochol, M., Jakubowska, K., Bendyk-Szeffer, M., Chlubek, D., & Buczkowska-Radlinska, J. (2018). Analysis of base monomer elution from 3 flowable bulk-fill composite resins using high performance liquid chromatography (HPLC). *Medical Science Monitor, 24*, 4679-4690.

Lambrechts, P., & Van Herle, G. (1982). Observation and comparison of polished composite surfaces with the aid of SEM and profilometer. *Journal of Oral Rehabilitation, 9*(3), 203-216.

Lee, M. J., Kim, M. J., Kwon, J. S., Lee, S. B., & Kim, K. M. (2017). Cytotoxicity of light-cured dental materials according to different sample preparation methods. *Materials (Basel), 10*(3), 288.

Lee, Y. K. (2008). Influence of filler on the difference between the transmitted and reflected colors of experimental resin composites. *Dental Materials, 24*(9), 1243-1247.

Leprince, J. G., Hadis, M., Shortall, A. C., Ferracane, J. L., Devaux, J., Leloup, G., & Palin, W. M. (2011). Photoinitiator type and applicability of exposure reciprocity law in filled and unfilled photoactive resins. *Dental Materials, 27*(2), 157-164.

Leprince, J. G., Palin, W. M., Hadis, M. A., Devaux, J., & Leloup, G. (2013). Progress in dimethacrylate-based dental composite technology and curing efficiency. *Dental Materials, 29*(2), 139-156.

Lindberg, A., Peutzfeldt, A., & van Dijken, J. W. (2005). Effect of power density of curing unit, exposure duration, and light guide distance on composite depth of cure. *Clinical Oral Investigations, 9*(2), 71-76.

Lovell, L. G., Newman, S. M., & Bowman, C. N. (1999). The effects of light intensity, temperature, and comonomer composition on the polymerization behavior of dimethacrylate dental resins. *Journal of Dental Research, 78*(8), 1469-1476.

Lutz, F., & Phillips, R. W. (1983). A classification and evaluation of composite resin systems. *Journal of Prosthetic Dentistry, 50*(4), 480-488.

Lutz, E., Krejci, I., & Oldenburg, T. R. (1986). Elimination of polymerization stresses at the margins of posterior composite resin restorations: a new restorative technique. *Quintessence International, 17*(12), 777-784.

Lutz, F., Krejci, I., & Barbakow, F. (1991). Quality and durability of marginal adaptation in bonded composite restorations. *Dental Materials, 7*(2), 107-113.

Malik, A. H., & Baban, L. M. (2014). The effect of light curing tip distance on the curing depth of bulk fill resin based composites. *Journal of Baghdad College of Dentistry, 26*(4), 46-53.

McCabe, J. F., & Ogden, A. R. (1987). The relationship between porosity, compressive fatigue limit and wear in composite resin restorative materials. *Dental Materials, 3*(1), 9-12.

McCabe, J. F., & Walls, A. W. G. (2008). *Applied Dental Materials* (Ninth ed.): Blackwell Publishing Ltd.

Meyer, G. R., Ernst, C. P., & Willershausen, B. (2002). Decrease in power output of new light-emitting diode (LED) curing devices with increasing distance to filling surface. *Journal of Adhesive Dentistry, 4*(3), 197-204.

Michaud, P. L., Price, R. B., Labrie, D., Rueggeberg, F. A., & Sullivan, B. (2014). Localised irradiance distribution found in dental light curing units. *Journal of Dentistry, 42*(2), 129-139.

Mitra, S. B., Wu, D., & Holmes, B. N. (2003). An application of nanotechnology in advanced dental materials. *Journal of the American Dental Association, 134*(10), 1382-1390.

Moharam, L. M., El-Hoshy, A. Z., & Abou-Elenein, K. (2017). The effect of different insertion techniques on the depth of cure and vickers surface micro-hardness of two bulk-fill resin composite materials. *Journal of Clinical and Experimental Dentistry, 9*(2), 266-271.

Moore, B. K., Platt, J. A., Borges, G., Chu, T. M., & Katsilieri, I. (2008). Depth of cure of dental resin composites: ISO 4049 depth and microhardness of types of materials and shades. *Operative Dentistry, 33*(4), 408-412.

Moorthy, A., Hogg, C. H., Dowling, A. H., Grufferty, B. F., Benetti, A. R., & Fleming, G. J. (2012). Cuspal deflection and microleakage in premolar teeth restored with bulk-fill flowable resin-based composite base materials. *Journal of Dentistry, 40*(6), 500-505.

Moszner, N., & Salz, U. (2001). New developments of polymeric dental composites. *Progress in Polymer Science, 26*(4), 535-576

Moszner, N., & Klapdohr, S. (2004). Nanotechnology for dental composites. *International Journal of Nanotechnology, 1*(1/2), 130-156.

Moszner, N., Fischer, U. K., Ganster, B., Liska, R., & Rheinberger, V. (2008). Benzoyl germanium derivatives as novel visible light photoinitiators for dental materials. *Dental Materials, 24*(7), 901-907.

Musanje, L., & Darvell, B. W. (2006). Curing-light attenuation in filled-resin restorative materials. *Dental Materials, 22*(9), 804-817.

Neumann, M. G., Schmitt, C. C., Ferreira, G. C., & Correa, I. C. (2006). The initiating radical yields and the efficiency of polymerization for various dental photoinitiators excited by different light curing units. *Dental Materials, 22*(6), 576-584.

Nocca, G., De Palma, F., Minucci, A., De Sole, P., Martorana, G. E., Calla, C., . . . Lupi, A. (2007). Alterations of energy metabolism and glutathione levels of HL-60 cells induced by methacrylates present in composite resins. *Journal of Dentistry, 35*(3), 187-194.

Opdam, N. J., Roeters, J. J., Joosten, M., & Veeke, O. (2002). Porosities and voids in Class I restorations placed by six operators using a packable or syringable composite. *Dental Materials, 18*(1), 58-63.

Pereira, A. G., Raposo, L., Teixeira, D., Gonzaga, R., Cardoso, I. O., Soares, C. J., & Soares, P. V. (2016). Influence of battery level of a cordless LED unit on the properties of a nanofilled composite resin. *Operative Dentistry, 41*(4), 409-416.

Peschke, A. (2013). *Tetric EvoCeram® Bulk Fill in clinical use*.

Peutzfeldt, A. (1997). Resin composites in dentistry: the monomer systems. *European Journal of Oral Sciences, 105*(2), 97-116.

Pires, J. A., Cvitko, E., Denehy, G. E., & Swift, E. J., Jr. (1993). Effects of curing tip distance on light intensity and composite resin microhardness. *Quintessence International, 24*(7), 517-521.

Price, R. B., Derand, T., Sedarous, M., Andreou, P., & Loney, R. W. (2000). Effect of distance on the power density from two light guides. *Journal of Esthetic Dentistry, 12*(6), 320-327.

Price, R. B., Felix, C. A., & Andreou, P. (2004). Effects of resin composite composition and irradiation distance on the performance of curing lights. *Biomaterials, 25*(18), 4465-4477.

Price, R. B., Labrie, D., Rueggeberg, F. A., & Felix, C. M. (2010). Irradiance differences in the violet (405 nm) and blue (460 nm) spectral ranges among dental light-curing units. *J Esthet Restor Dent, 22*(6), 363-377.

Price, R. B., Rueggeberg, F. A., Harlow, J., & Sullivan, B. (2016). Effect of mold type, diameter, and uncured composite removal method on depth of cure. *Clinical Oral Investigations, 20*(7), 1699-1707.

Rode, K. M., Kawano, Y., & Turbino, M. L. (2007). Evaluation of curing light distance on resin composite microhardness and polymerization. *Operative Dentistry, 32*(6), 571-578.

Roggendorf, M. J., Kramer, N., Appelt, A., Naumann, M., & Frankenberger, R. (2011). Marginal quality of flowable 4-mm base vs. conventionally layered resin composite. *Journal of Dentistry, 39*(10), 643-647.

Roulet, J. F., Rocha, M. G., Shen, C., Khudhair, M. M., & Oliveira, D. C. (2018). Beam profile characterization of a dental light curing unit using a spectrometer-based method. *Stomatology edy Journal, 5*(2), 84-91.

Rueggeberg, F. A., & Craig, R. G. (1988). Correlation of parameters used to estimate monomer conversion in a light-cured composite. *Journal of Dental Research, 67*(6), 932-937.

Rueggeberg, F. A., & Margeson, D. H. (1990). The effect of oxygen inhibition on an unfilled/filled composite system. *Journal of Dental Research, 69*(10), 1652-1658.

Rueggeberg, F. (1999). Contemporary issues in photocuring. *Compendium of Continuing Education in Dentistry Supplement* (25), S4-15; quiz S73.

Rueggeberg, F. A. (2011). State-of-the-art: dental photocuring--a review. *Dental Materials, 27*(1), 39-52.

Ruyter, I. E., & Oysaed, H. (1982). Conversion in different depths of ultraviolet and visible light activated composite materials. *Acta Odontologica Scandinavica, 40*(3), 179-192.

Ruyter, I. E., & Oysaed, H. (1987). Composites for use in posterior teeth: composition and conversion. *Journal of Biomedical Materials Research, 21*(1), 11-23.

Schmitt, W., Purrmann, R., Jochum, P., & Hubner, H.-J. (1981). Use of silicic acid pellets as fillers for dental materials. Patent WO 81/01366-PCT/EP 80/00135.

Schneider, L. F., Pfeifer, C. S., Consani, S., Prahl, S. A., & Ferracane, J. L. (2008). Influence of photoinitiator type on the rate of polymerization, degree of conversion, hardness and yellowing of dental resin composites. *Dental Materials, 24*(9), 1169-1177.

Schneider, L. F., Cavalcante, L. M., Consani, S., & Ferracane, J. L. (2009). Effect of co-initiator ratio on the polymer properties of experimental resin composites formulated with camphorquinone and phenyl-propanedione. *Dental Materials, 25*(3), 369-375.

Schulze, S., & Vogel, H. (1998). Aspects of the Safe Storage of Acrylic Monomers: Kinetics of the Oxygen Consumption. *Chemical Engineering & Technology, 21*(10), 829-837.

Shibasaki, S., Takamizawa, T., Nojiri, K., Imai, A., Tsujimoto, A., Endo, H., . . . Miyazaki, M. (2017). Polymerization behavior and mechanical properties of high-viscosity bulk fill and low shrinkage resin composites. *Operative Dentistry, 42*(6), 177-187.

Shortall, A. C., Palin, W. M., & Burtscher, P. (2008). Refractive index mismatch and monomer reactivity influence composite curing depth. *Journal of Dental Research, 87*(1), 84-88.

Shortall, A. C., Felix, C. J., & Watts, D. C. (2015). Robust spectrometer-based methods for characterizing radiant exitance of dental LED light curing units. *Dental Materials, 31*(4), 339-350.

Shortall, A. C., Price, R. B., MacKenzie, L., & Burke, F. J. (2016). Guidelines for the selection, use, and maintenance of LED light-curing units - Part 1. *British Dental Journal, 221*(8), 453-460.

Singhal, S., Gurtu, A., Singhal, A., Bansal, R., & Mohan, S. (2017). Effect of different composite restorations on the cuspal deflection of premolars restored with different insertion techniques- an in vitro study. *Journal of Clinical Diagnostic Research, 11*(8), 67-70.

Skeeters, T. M., Timmons, J. G., & Mitchell, R. J. (1983). Curing Depth of Visible Light Cured Composite Resin. *Journal of Dental Research, 62*, 219, (Abstract No. 448)

Sobrinho, L. C., Goes, M. F., Consani, S., Sinhoreti, M. A., & Knowles, J. C. (2000). Correlation between light intensity and exposure time on the hardness of composite resin. *Journal of Materials Science: Materials in Medicine, 11*(6), 361-364.

Stansbury, J. W. (2000). Curing dental resins and composites by photopolymerization. *Journal of Esthetic Dentistry, 12*(6), 300-308.

Stansbury, J. W., Trujillo-Lemon, M., Lu, H., Ding, X., Lin, Y., & Ge, J. (2005). Conversion-dependent shrinkage stress and strain in dental resins and composites. *Dental Materials, 21*(1), 56-67.

Sun, G. J., & Chae, K. H. (2000). Properties of 2,3-butanedione and 1-phenyl-1,2-propanedione as new photosensitizers for visible light cured dental resin composites. *Polymer, 41*(16), 6205-6212.

Thome, T., Steagall, W., Jr., Tachibana, A., Braga, S. R., & Turbino, M. L. (2007). Influence of the distance of the curing light source and composite shade on hardness of two composites. *Journal of Applied Oral Science, 15*(6), 486-491.

Tongtaksin, A., & Leevailoj, C. (2017). Battery charge affects the stability of light intensity from light-emitting diode light-curing units. *Operative Dentistry, 42*(5), 497-504.

Truffier-Boutry, D., Demoustier-Champagne, S., Devaux, J., Biebuyck, J. J., Mestdagh, M., Larbanois, P., & Leloup, G. (2006). A physico-chemical explanation of the post-polymerization shrinkage in dental resins. *Dental Materials, 22*(5), 405-412.

Uhl, A., Sigusch, B. W., & Jandt, K. D. (2004). Second generation LEDs for the polymerization of oral biomaterials. *Dental Materials, 20*(1), 80-87.

Vandewalle, K. S., Roberts, H. W., Andrus, J. L., & Dunn, W. J. (2005). Effect of light dispersion of LED curing lights on resin composite polymerization. *Journal of Esthetic and Restorative Dentistry, 17*(4), 244-254.

Vankerckhoven, H., Lambrechts, P., van Beylen, M., & Vanherle, G. (1981). Characterization of composite resins by NMR and TEM. *Journal of Dental Research, 60*(12), 1957-1965.

Vankerckhoven, H., Lambrechts, P., van Beylen, M., Davidson, C. L., & Vanherle, G. (1982). Unreacted methacrylate groups on the surfaces of composite resins. *Journal of Dental Research, 61*(6), 791-795.

Versluis, A., Douglas, W. H., Cross, M., & Sakaguchi, R. L. (1996). Does an incremental filling technique reduce polymerization shrinkage stresses? *Journal of Dental Research, 75*(3), 871-878.

Xia, W. Z., & Cook, W. D. (2003). Exotherm control in the thermal polymerization of nona-ethylene glycol dimethacrylate (NEGDM) using a dual radical initiator system. *Polymer, 44*(1), 79-88.

Yap, A. U., & Seneviratne, C. (2001). Influence of light energy density on effectiveness of composite cure. *Operative Dentistry, 26*(5), 460-466.

Yap, A. U., Wong, N. Y., & Siow, K. S. (2003). Composite cure and shrinkage associated with high intensity curing light. *Operative Dentistry, 28*(4), 357-364.

Yap, A. U., Tan, C. H., & Chung, S. M. (2004). Wear behavior of new composite restoratives. *Operative Dentistry, 29*(3), 269-274.

Yokesh, C. A., Hemalatha, P., Muthalagu, M., & Justin, M. R. (2017). Comparative evaluation of the depth of cure and degree of conversion of two bulk fill flowable composites. *Journal of Clinical Diagnostic Research, 11*(8), 86-89.

LIST OF PUBLICATIONS AND PAPERS PRESENTED

Diab, R. A., Yahya N. A., Gonzalez M. A. G., Yap A. U., (2019, March). *Effect of Curing Light Distance on the Cure of Bulk-Fill Composite Resins.* 18th Annual Scientific Meeting & 20th Annual General Meeting of IADR, Malaysian Section, Kuala Lumpur, Malaysia.